Published in final edited form as:
Alcohol Clin Exp Res. 2011 May ; 35(5): 885–904. doi:10.1111/j.1530-0277.2010.01419.x.

Ethanol exposure in early adolescence inhibits intrinsic neuronal plasticity via sigma-1 receptor activation in hippocampal CA1 neurons

Jilla Sabeti
Department of Molecular and Integrative Neurosciences, The Scripps Research Institute, La Jolla, California and Center for Development and Behavioral Neuroscience, Department of Psychology, State University of New York at Binghamton, NY

Abstract

Background—We demonstrated previously that rats exposed to chronic intermittent ethanol (CIE) vapors in early adolescence show increased magnitudes of long-term potentiation (LTP) of excitatory transmission when recorded at dendritic synapses in hippocampus. Large amplitude LTP following CIE exposure is mediated by sigma-1 receptors; however, not yet addressed is the role of sigma-1 receptors in modulating the intrinsic properties of neurons to alter their action potential firing during LTP.

Methods—Activity-induced plasticity of spike firing was investigated using rat hippocampal slice recordings to measure changes in both field excitatory postsynaptic potentials (fEPSPs) and population spikes (pop. spikes) concomitantly at dendritic inputs and soma of CA1 pyramidal neurons, respectively.

Results—We observed unique modifications in plasticity of action potential firing in hippocampal slices from CIE exposed adolescent rats, where the induction of large amplitude LTP by 100 Hz stimulations was accompanied by reduced CA1 neuronal excitability—reflected as decreased pop. spike efficacy and impaired activity-induced fEPSP-to-spike (E-S) potentiation. By contrast, LTP induction in ethanol-naïve control slices resulted in increased spike efficacy and robust E-S potentiation. E-S potentiation impairments emerged at 24 hr after CIE treatment cessation, but not before the alcohol withdrawal period, and were restored with bath-application of the sigma-1 receptor selective antagonist BD1047, but not the NMDA receptor antagonist D-AP5. Further evidence revealed a significantly shortened somatic fEPSP time course in adolescent CIE-withdrawn hippocampal slices during LTP; however, paired-pulse data show no apparent correspondence between E-S dissociation and altered recurrent feedback inhibition.

Conclusions—Results here suggest that acute withdrawal from adolescent CIE exposure triggers sigma-1 receptors that act to depress the efficacy of excitatory inputs in triggering action potentials during LTP. Such withdrawal-induced depression of E-S plasticity in hippocampus likely entails sigma-1 receptor modulation of one or several voltage-gated ion channels controlling the neuronal input-output dynamics.

Keywords

Chronic intermittent ethanol; adolescence; sigma-1 receptors; plasticity; EPSP-spike (E-S) coupling

Correspondence: Dr. Jilla Sabeti, Department of Psychology, State University of New York at Binghamton, P.O. Box 6000, Vestal Parkway East, Binghamton, NY 13902-6000, USA. Phone: (607) 777-4219; FAX: (607) 777-4890; jsabeti@binghamton.edu.

Introduction

The abuse of alcohol during the adolescent window of development can lead to persistent neurobehavioral deficits where memory dysfunction is prominent (Brown et al., 2000; Land and Spear, 2004). In animal models, both acute and chronic alcohol exposure inhibits long-term potentiation (LTP) of excitatory neurotransmission in hippocampus (Durand and Carlen, 1984; Morrisett and Swartzwelder, 1993; Roberto et al., 2002; Schummers et al., 1997; Sinclair and Lo, 1986; Tokuda et al., 2007), which is considered a major synaptic mechanism underlying alcohol-related memory loss (White et al., 2000) and perhaps also alcohol addiction (Carpenter-Hyland and Chandler, 2007). We demonstrated recently that binge-like alcohol exposure via chronic intermittent ethanol (CIE) vapor inhalation in early-stage adolescent rats results instead in increased LTP amplitudes at hippocampal CA3-CA1 dendritic inputs—whereas the same CIE treatment in late-stage adolescent animals leads to typical LTP depression at the same synapses (Sabeti and Gruol, 2008). Such bi-directional change in LTP by alcohol actions across the early-to-late stages of adolescent development suggests that additional neuronal modifications beyond the change in synaptic strength likely account for the negative outcomes of early life alcohol abuse on memory and neurobehavioral functioning.

Increasing appreciation for the nonsynaptic aspects of plasticity has prompted studies investigating intrinsic changes in the firing probability or excitability of neurons with LTP (Turrigiano and Nelson, 2004; Zhang and Linden, 2003). For example, early reports indicate that LTP induction modifies the neuronal properties of synaptic integration such that neurons fire more readily at any given excitatory input (Abraham et al., 1987; Andersen et al., 1980; Taube and Schwartzkroin, 1988)—a process referred to as excitatory postsynaptic potential-to-spike coupling (EPSP-spike or E-S) potentiation. Activity-induced E-S potentiation in hippocampus reflects increased neuronal excitability through selective modifications in the magnitude of voltage-dependent currents (Campanac et al., 2008; Daoudal et al., 2002; Wang et al., 2003; Xu et al., 2005) and/or reduced GABA inhibitory transmission (Abraham et al., 1987; Chavez-Noriega et al., 1989; Staff and Spruston, 2003). By contrast, afferent stimulations that elicit large LTP amplitudes above optimal levels reportedly decrease neuronal excitability through altered activity of voltage-gated ion channels that undergo feedback regulation (Fan et al., 2005). The question investigated here is whether the large amplitude LTP associated with early adolescent CIE exposure (Sabeti and Gruol, 2008) leads to inhibited E-S potentiation in area CA1, thereby accounting for altered signal transfer thru hippocampus.

Two independent pathways mediate the up- or down-regulation of LTP by chronic alcohol vapor inhalation: a conventional postsynaptic NMDA receptor pathway in the case for LTP depression (Nelson et al., 2005; Roberto et al., 2002; Sabeti and Gruol, 2008) and a non-NMDA receptor pathway involving sigma-1 receptor actions in the case for LTP augmentation (Sabeti and Gruol, 2008). Sigma-1 receptors are ligand-regulated receptors endogenous to several brain regions, including the hippocampus, hypothalamus, and cerebral cortex (Alonso et al., 2000), which subserve learning, memory and emotion. While the central administration of sigma-1 receptor agonists alone largely fails to affect learning/memory in normal control animals, their administration in amnesic animal models appears to effectively rescue memory deficits induced by blockade of glutamatergic or cholinergic systems (Maurice and Su, 2009). Likewise, sigma-1 receptor selective antagonists are reported to reverse the mnemonic impairments induced by alcohol exposure (Meunier et al., 2006), as well as reduce alcohol drinking (Sabino et al., 2009), and block alcohol-induced conditioned place preference (Maurice et al., 2003).

At the cellular level in brain and oocytes, sigma-1 receptors act to predominately inhibit one or several voltage-sensitive conductances through ligand-directed (Cheng et al., 2008; Martina et al., 2007; Zhang and Cuevas, 2002; Zhang and Cuevas, 2005) and/or protein-protein (Aydar et al., 2002; Hayashi and Su, 2001) interactions with their known ion channel effectors. A functional induction of sigma-1 receptors by alcohol or other abused drugs (Meunier et al., 2006; Stefanski et al., 2004) would suggest also their potential role in drug-induced modulation of intrinsic (voltage-gated) neuronal plasticity. The present study investigates induced changes in E-S coupling by using extracellular recordings of population responses obtained simultaneously from both the dendritic and somatic regions of CA1 pyramidal neurons. The extracellular approach enabled us to capture a marked inhibition of E-S plasticity arising from increased sigma-1 receptor activation in acute abstinence from adolescent CIE exposure.

Materials and Methods

Animals

Animal care and use procedures were in strict accordance with NIH guidelines and approved by the Institutional Animal Care and Use Committee and the Animal Research Committee at the Scripps Research Institute. Male Wistar rats (26-37 postnatal days old, or in early-stage adolescence, at the start of experiments; Charles River Laboratories) were housed 2-3 per cage with food and water made available ad libitum throughout the CIE vapor or air inhalation period. Rats were allowed to acclimate to their home-cage for 1-2 days prior to start of experiments.

CIE vapor treatments

Designed for modeling binge-like alcohol exposure (O'Dell et al., 2004), the CIE vapor inhalation paradigm was utilized for its reported efficacy in producing ethanol-dependence in genetically heterogeneous rats (O'Dell et al., 2004; Slawecki et al., 2004) and promoting lasting synaptic plasticity changes in hippocampus (Nelson et al., 2005; Sabeti and Gruol, 2008). Briefly, rats in their home-cage were placed in sealed inhalation chambers (La Jolla Alcohol Research Inc.) where they were exposed to either 95% ethanol vapors (CIE treatment group) or air (naïve control group) on a chronic intermittent schedule, which consisted of daily exposure occurring on a 14 h on/10 h off cycle, repeated consecutively for 14 days as described previously (Sabeti and Gruol, 2008). Control and CIE treatment groups were matched for age such that at the start of treatments on Day 1, all rats were in the early-stage of adolescent development at 26-37 days old before puberty onset (Spear, 2000). At treatment termination on Day 14 when recordings were made, all rats had advanced in age towards early post-pubescence or late-stage adolescence (Spear, 2000).

Ethanol vapor concentrations were adjusted to maintain a target blood ethanol concentration of 150-200 mg/dL that was assessed by tail bleed at least twice per week, as described previously in detail (O'Dell et al., 2004). Mean blood ethanol concentrations on Days 1-14 were 187 ± 10 mg/dL in CIE-treated rats (n = 28) and negligible in naïve control rats (n = 14). Immediately after the vapor exposure period ended on Day 14, a subset of the CIE-treated rats was sacrificed for brain slice recordings while their blood alcohol levels were elevated (170 ± 14 mg/dL, CIE non-withdrawn, n = 14 rats). The remaining CIE-treated animals were sacrificed after being housed for an additional 24 h in their home-cage within another inhalation chamber that did not receive ethanol vapors, such that blood alcohol concentrations dropped to negligible levels prior to sacrifice for recordings (CIE-withdrawn, n = 14 rats).

Acute hippocampal slice preparations

Rats were deeply anesthetized by exposure to halothane vapors prior to sacrifice. After the loss of tail- and paw-pinch reflexes was observed, rats were decapitated, brains quickly removed, and the hippocampi dissected. Transverse 400 μm thick slices of the dorsal hippocampus were made using a tissue chopper (Mickle Laboratory Engineering, Surrey, UK). During dissection procedures, brains were immersed in ice-cold and carboxygenated (95% O_2 and 5% CO_2; pH 7.2-7.4; Air Gas, San Diego, CA) artificial cerebral spinal fluid (ACSF) that was modified to contain high-Mg^{2+} and low-Ca^{2+} concentrations: (in mM) 5.0 $MgS0_4$, 0.2 $CaCl_2$, 130 NaCl, 3.5 KCl, 1.25 NaH_2PO_4, 24 $NaHCO_3$ and 10 glucose. Slices were maintained and recorded in warm (33°C ± 1°C) and carboxygenated ACSF containing physiological concentrations of Mg^{2+} and Ca^{2+} ions: (in mM) 1.0 $MgS0_4$, 2.0 $CaCl_2$ and the same concentrations of the other salts listed above. Slices from the non-withdrawn CIE group were maintained in ACSF containing ethanol at 150 mg/dL, with continuous perfusion throughout the recording period, to prevent potential ethanol withdrawal effects; and slices from naïve and CIE-withdrawn animals were maintained and recorded in the absence of ethanol in the bath solution.

Extracellular electrophysiological recordings

Hippocampal slices were quickly transferred from an interface chamber where they were maintained for at least 1 h (ACSF flow rate: 0.55 ml/min) to a second interface chamber for recording (flow rate: 2.0 ml/min). A micro-concentric bipolar stimulating electrode (150 μm outer contact diameter; 25 μm inner contact diameter; 50 mm shaft; Rhodes Medical Instruments, Summerland, CA) was positioned slowly under visual control onto the CA3 Schaffer collateral afferent fibers. Recording glass electrode-pipettes (2-3 MΩ; World Precision Instruments, Inc., Sarasota, FL) were filled with normal ACSF and positioned under visual control within both the stratum radiatum (apical dendritic layer) and the stratum pyramidale (somatic layer) of area CA1 neurons by the aid of micro-manipulators (MP-225 and MP285, Sutter Instrument Company, Novato, CA). Electrical stimulations were relayed to the stimulating electrode by a constant-voltage stimulus isolation unit (Grass SIU Model 5, Quincy, MA). Evoked signals were amplified using the Axoclamp 2A amplifier (Axon Instruments, Foster City, CA). Data were acquired using the pClamp software program (v. 8.2, Axon Instruments). Recordings in slices from either naïve control (air) or CIE-treated animals were made on alternating days. Stimulation protocols were run in the order described below.

Stability tests—Before the start of experiments, concurrently recorded dendritic and somatic responses to test electrical stimulations (i.e., field potentials and spikes) were monitored for stability for 15-30 min. Data were collected only from slices that (1) exhibited field excitatory postsynaptic potential (fEPSP) peak amplitudes ≥ 1 mV and a single population spike (pop. spike) at the maximal stimulation voltage tested; and (2) showed strong paired-pulse evoked inhibition in the pop. spike amplitude by at least 30-40% (10 ms inter-stimulus interval), indicating intact recurrent inhibitory function (Meyer et al., 1999; Steffensen and Henriksen, 1991). These criteria helped minimize differences between slices from the various preparations and ensured that compromised slices undergoing damage during storage/preparation procedures were excluded from analysis (Roberto et al., 2002). The percentage of slices that failed to meet criteria was minimal (~20-25%) and did not differ between treatment groups.

Input-output protocol—Single-pulse test stimulations from low-to-high voltage strengths were delivered every 30 s in 2 V increments, starting at the near-threshold voltage for eliciting a measurable fEPSP slope or pop. spike amplitude and continuing until voltages eliciting maximal response magnitudes were obtained. The protocol was repeated both

before (baseline) and again at 60 min after LTP induction in individual slices. At baseline prior to LTP induction, slices from the different treatment groups exhibited similar relationships between the applied stimulus voltage and evoked response magnitudes when tested across a wide range of stimulation intensities. For example, applied stimulus voltages eliciting threshold pop. spike responses (i.e., defined as the first measurable pop. spike amplitude ≥ 0.5 mV) were similar for the slices recorded (mean threshold stimulus voltage: naïve 12 ± 2 V; CIE-withdrawn 10 ± 1 V; and CIE non-withdrawn, 11 ± 1 V, n = 21, 21 and 16 slices, respectively), with mean threshold pop. spike amplitudes that did not differ significantly between the three treatment groups (threshold pop. spike amplitudes: naïve 1.4 ± 0.1 mV, CIE-withdrawn 1.7 ± 0.2 mV, and CIE non-withdrawn, 1.5 ± 0.2 mV). No significant treatment group differences were found in the maximal pop. spike amplitudes at baseline (naïve 11.6 ± 0.8 mV; CIE-withdrawn 10.4 ± 0.6 mV; and CIE-non-withdrawn 10.3 ± 0.4 mV, n = 21, 21, and 16 slices, respectively) nor in the maximally required stimulus intensities (mean maximal stimulus voltage: naïve 22 ± 2 V; CIE-withdrawn 20 ± 1 V; CIE non-withdrawn 20 ± 2 V). Likewise naïve and CIE-withdrawn slices showed similar evoked fEPSP magnitudes at dendritic inputs over a wide range of stimulus voltages tested at baseline, as previously illustrated in detail (Sabeti and Gruol, 2008).

Paired-pulse evoked inhibition—The paired-pulse stimulation paradigm entailed stimulating the CA3 Schaffer collateral afferent fibers by two consecutive pulses separated by a 10 ms interval (Sabeti et al., 2007). Paired-pulse stimulations were applied using (1) the maximal stimulation voltage to ensure full activation of the trisynaptic circuit mediating feedback inhibition in CA1 or (2) a lower stimulation voltage as indicated to minimize the possible contribution of Na^+ channel inactivation and/or presynaptic depletion as potential factors underlying evoked inhibition (Zucker and Regehr, 2002). The decrease in the amplitude of the second compared to the first evoked pop. spike (i.e., paired-pulse inhibition level) is considered to reflect short-term activation of the inhibitory feedback circuit impinging onto CA1 pyramidal neurons (Meyer et al., 1999; Steffensen and Henriksen, 1991).

Where indicated in some paired-pulse experiments, the neurosteroid 3α-hydroxy-5β-pregnan-20-one sulfate (3α5β sulfate; 5 μM) was bath applied prior to recordings. The rationale for use of 3α5β sulfate are results from studies in cultured hippocampal neurons indicating negative modulation of GABA-A receptor mediated responses by 3α5β sulfate at high nanomolar to micromolar concentrations (Mennerick et al., 2008; Park-Chung et al., 1999; Wang et al., 2002), in contrast to the channel blocking actions of picrotoxin. At the 5 μM concentration tested here, 3α5β sulfate bath-application (30 min perfusion period) did not interfere with the pop. spike shape so that the change in paired-pulse inhibition levels with LTP could be evaluated in the continued presence of 3α5β sulfate in the bath solution. By comparison, bath-application of the GABA-A receptor channel blocker picrotoxin (100 μM) resulted in the elicitation of multiple pop. spikes that distorted the fEPSP waveforms, thereby precluding its use in paired-pulse inhibition studies. Unless otherwise indicated, data are the percentage change in paired-pulse inhibition levels from baseline at 60 min after or in the absence of the 100 Hz tetanus stimulations on the basis of within-slice comparisons.

LTP protocol—The LTP induction protocol always consisted of delivering 3 trains of high-frequency tetanus stimulations (100 Hz, 1 s duration, 20 s inter-train interval) to the Schaffer collateral fibers, using a stimulus voltage intensity producing ~35-45% of the maximal fEPSP response amplitude at baseline, as described previously (Sabeti and Gruol, 2008). After a 20 s delay following the last tetanus train, responses continued to be sampled by applying test stimulations once every min for an additional 60 min, using the same stimulus voltage applied at baseline. Slices were considered to show LTP if the dendritic fEPSP slope remained elevated at >125% of the baseline slope for at least 55-60 min

following tetanus application. Tetanus stimulations were delivered only after the establishment of steady baseline measurements, which were taken as the mean of five consecutive responses (i.e., fEPSP slopes and pop. spike amplitudes) sampled every min over a 5 min period immediately prior to tetanus application. In most cases, the test stimulation voltage required to produce the near half-maximal fEPSP amplitude at baseline was below the threshold for eliciting a measurable pop. spike amplitude. Therefore, for some experiments, the test stimulation voltage was increased initially to elicit a pop. spike of either threshold amplitude (≥ 0.5 mV) or near half-maximal amplitude (35-45% of the maximal response); thus, the ratio between the second (post-tetanus) to the first (pretetanus) pop. spike amplitude evoked by the same test stimulus voltage could be determined for individual slices. High frequency input stimulations in the ~100 Hz ranges is suggestively of relevance to behavior in physiological states in that it may elicit fast oscillations in hippocampal networks as found during exploratory behaviors or intense mental activity, for instance (Lisman, 2005; Whittington et al., 2000).

Data and statistical analysis

fEPSP and pop. spike waveforms were analyzed using the AxoGraph software program (v. 4.6, Axon Instruments). The maximal slope of the dendritically recorded fEPSP waveform was determined over the initial 40-60% range of the rising phase of the evoked fEPSP and used as an indicator of field synaptic activity (depolarization) near the site of stimulation (Nelson et al., 2005; Sabeti et al., 2007). The amplitude of the somatically recorded pop. spike—appearing as a large negative wave superimposed on the positive rising phase of the incoming fEPSP—was measured from the maximum downward deflection to the peaks in the rising component of the somatic fEPSP (Nelson et al., 2005). The pop spike amplitude was used as an indicator for active discharge (output) of a population of synchronously firing neurons.

Input-output parameters of synaptic transmission were evaluated by plotting the pop. spike amplitude (output) against the concurrently recorded incoming dendritic fEPSP slope (input) to generate EPSP-to-spike (E-S) curves. E-S plots were fit to the Boltzmann sigmoidal equation: $Y = Top / (1 + \exp((E_{50} - X)/slope))$, where Y is the evoked pop. spike amplitude, Top is the fitted maximum pop. spike amplitude, X is the measured incoming dendritic fEPSP slope, and E_{50} is the fitted fEPSP slope that gives rise to the half-maximal pop. spike amplitude. Thus, the E_{50} value represents the efficacy of the fEPSP input for eliciting a pop. spike within the recorded field. Frequency histogram plots were generated for the change in the E_{50} value over time by recording the number of slices that fell within each response magnitude indicated (i.e., unit of change in the E_{50} value from baseline). Histogram plots were fit to the Gaussian distribution equation using the GraphPad Prism software program (v. 5c) to determine deviations from the normal distribution (R^2 = 0.9452-0.9947).

Decay tau values (i.e., mean lifetime) were determined by fitting the decaying portion of the dendritic or somatic fEPSP waveform to a single-phase exponential decay function (R^2 = 0.9631-0.9981). Data were fit from the peak amplitude of the evoked fEPSP to its bottom plateau value at or near zero over a ~52 ms interval. To eliminate distortion of the fEPSP waveform by the presence of a pop. spike, which could potentially interfere with kinetic measurements, only fEPSP waveforms were selected that were near and below the threshold for action potential generation, with fEPSP magnitudes that were similar across the three treatment groups in the sample data set used for analysis (dendritic fEPSP slope: Naive 1.3 ± 0.1 mV/ms, n =12 slices; CIE non-withdrawn 1.3 ± 0.1 mV/ms, n = 9 slices; CIE-withdrawn 1.1 ± 0.1 mV/ms, n = 9 slices).

One- or two-way ANOVA calculations were run followed by either one sample t-tests or Bonferroni post-tests corrected for multiple comparisons. A level of $p < 0.05$ is considered

significant. Curve fitting and statistical analyses were performed using the GraphPad Prism software program (v. 5c GraphPad Software Inc., San Diego, CA).

Drugs

Drugs were prepared as concentrated stock solutions and diluted to the indicated working concentration by addition to the flow of the superfusing fluid (i.e., normal ACSF medium). Stock solutions of D-(-)-2-amino-5-phosphonopentanoic acid (D-AP5) and BD1047 dihydrobromide were prepared as 1000 x the final concentration in distilled water and stored at −80 °C until the experimental day. Stock solutions of 3α5β sulfate and pregnenolone sulfate were prepared on the experimental day at 1 mg/ml by sonication in distilled water. D-AP5 and BD1047 dihydrobromide were purchased from Tocris Cookson Inc. (Ellisville, MO) and the neurosteroids 3α5β sulfate and pregnenolone sulfate were provided generously by Dr. Robert H. Purdy (The Scripps Research Institute, La Jolla, CA). All other reagents were purchased from Sigma (St. Louis, MO).

Results

Early adolescent alcohol exposure inhibits activity-induced E-S plasticity in hippocampus

Comparisons of dendritic versus somatic LTP responses in area CA1—We reported previously (Sabeti and Gruol, 2008) and show here in Fig. 1A that CIE exposure via ethanol vapor inhalation in early-stage adolescent rats, with subsequent 24 hr withdrawal from ethanol, substantially increases LTP levels at CA3–CA1 dendritic synapses, as compared to control LTP levels in age-matched naïve animals. Therefore, we investigated here the impact of increased LTP following early-adolescent CIE exposure on the firing activity of CA1 neurons, which provide one of the main excitatory projections from hippocampus. A dual extracellular recording configuration was utilized to simultaneously measure fEPSPs and pop. spikes respectively at both the dendritic and somatic layers of CA1 neurons in dissected hippocampal slice preparations. For initial experiments, hippocampal slices were prepared at 24 hr after CIE treatment termination and, hence, designated CIE-withdrawn slices.

Following the establishment of steady evoked responses at baseline, LTP was induced by high-frequency stimulations (100 Hz, 3 trains, 20 s inter-train intervals, 1 s duration per train at 35-45% of the maximal stimulus voltage) of the excitatory Schaffer collateral inputs near the apical dendrites of CA1 neurons. The multiple 100 Hz trains optimize the likelihood of LTP successes under control conditions and are shown to effectively differentiate between early adolescent versus late adolescent CIE exposure effects on synaptic LTP and non-NMDA receptor mediated plasticity pathways (Sabeti and Gruol, 2008).

At the dendritic recording site, delivery of the 100 Hz tetanus stimulations resulted in significant potentiation in the evoked fEPSP magnitude above baseline, which persisted for at least 60 min in both naïve control and CIE-withdrawn hippocampal slices (Fig. 1A, dendritic fEPSP slope: Naive 154 ± 15% of baseline and CIE-withdrawn 220 ± 16% of baseline, n = 10 slices each at 60 min post-tetanus; $p < 0.01$ versus 100% of baseline for each group by a one sample t-test). LTP of the dendritic fEPSP magnitude was increased substantially by ~40% in CIE-withdrawn slices, as compared to naïve controls (Fig. 1A, second set of columns; $p < 0.05$ Naive versus CIE-withdrawn). These findings are in agreement with our previous study demonstrating robust facilitation of LTP at CA1 dendritic synapses after early adolescent CIE exposure (Sabeti and Gruol, 2008).

In recordings obtained simultaneously from the somatic region of CA1 neurons, the same 100 Hz tetanus applied to the Schaffer collateral fibers likewise triggered an increase in the

evoked pop. spike amplitude, which persisted for at least 60 min in both naïve and CIE-withdrawn slices, consistent with a robust pop. spike-LTP response (Fig. 1B, pop. spike amplitude: Naive 210 ± 20% of baseline and CIE-withdrawn 230 ± 30% of baseline, n = 10 slices each at 60 min post-tetanus, $p < 0.01$ versus 100% of baseline for each group by a one sample t-test). However, CIE-withdrawn slices showed no appreciable enhancement in the pop. spike-LTP magnitude above that in naïve slices (Fig. 1B). For these analyses, LTP was evaluated using a test stimulation voltage that evoked a near half-maximal pop. spike amplitude at baseline (Fig. 1B). However, we likewise found no significant differences in the pop. spike-LTP levels between naïve and CIE-withdrawn slices when LTP was evaluated at a lower test stimulus intensity that evoked only a threshold pop. spike amplitude at baseline (mean pop. spike amplitude increase: Naive 7.9 ± 1.3 fold-increase from baseline and CIE-withdrawn 7.8 ± 1.3 fold-increase from baseline, n = 10 slices each at 60 min post-tetanus; $p < 0.001$ versus no change from baseline or a ratio of 1 for each group by a one sample t-test).

Finally, in experiments when the 100 Hz tetanus trains were omitted, no significant change was detected for at least 60 min in the concomitantly recorded fEPSP (Fig. 1A) and pop. spike amplitudes (Fig. 1B) in any of the slices recorded, demonstrating the dependence of both dendritic and somatic LTP responses on synaptic activation by the tetanus stimulations. Together these results indicate that LTP facilitation by CIE treatment in early adolescence appears to be spatially restricted to CA1 dendritic inputs and not necessarily accompanied by an enhancement in the pop. spike LTP response at CA1 soma.

Inhibition of E-S potentiation during LTP in CIE-withdrawn hippocampal slices —LTP in the pop. spike amplitude reflects an increased number of synchronously firing neurons attributed to: (1) direct effects of the increasing EPSP size itself, such that now more synapses reach the spike threshold amplitude and/or (2) activity-induced change in neuronal excitability, resulting in increased firing probability at any given input strength. Therefore, we considered the possibility that the firing probability of CA1 neurons is modulated by LTP in a distinct manner in CIE-withdrawn as compared to naive slices, thereby accounting for the similar pop. spike-LTP magnitudes in all slices (Fig. 1B), even in the face of the greater incoming fEPSP potentiation in the CIE-withdrawn slices recorded (Fig. 1A).

To evaluate the impact of LTP induction on the action potential firing probability of CA1 neurons we subjected a larger data set to E-S coupling analyses where pop. spike amplitudes were plotted as a function of their corresponding fEPSP magnitudes. Such analyses yielded the E_{50} parameter representing the efficacy of excitatory inputs in triggering action potentials. Analysis of the E-S coupling relationship in naïve slices revealed that LTP induction by the 100 Hz tetanus stimulations resulted in a prominent leftward shift in the E-S curve, or a negative change in the E_{50} from baseline, hence referred to as E-S potentiation (Fig. 2A, C, E). This is illustrated in Fig. 2C for an individual naïve slice, which exhibits increased pop. spike amplitudes for any given magnitude of the incoming fEPSP at 60 min after tetanization, relative to responses prior to LTP induction. The data suggested a substantial tetanus-induced increase in the pop. spike amplitude beyond that accounted for by the growing fEPSP magnitude in the naïve slice. By contrast, CIE-withdrawn slices generally showed a lack of a leftward displacement or no E-S potentiation at 60 min after tetanization (Fig. 2B, D, E), suggesting that the increase in the pop. spike amplitude during LTP reflected no more than the increased dendritic fEPSP size (Fig. 2D).

The frequency distribution of the E_{50} values after relative to before LTP induction was evaluated for the naïve and CIE-withdrawn group of slices recorded. In naïve slices, the peak of the distribution showed a statistically significant negative change in the E_{50} at 60

min after tetanization, indicative of a shift towards E-S potentiation with LTP in the majority of cases recorded (Fig. 2E, n = 14 out of 21 slices; mean E_{50} difference: −18.4 ± 3.0 % from baseline; $p < 0.001$ versus zero change at 60 min post-tetanus by a one sample t-test). Thus, only a small percentage of naïve slices recorded showed a positive change in the E_{50} with LTP, which is concluded to be due to normal variance in the response as would be predicted by a Gaussian distribution (Fig. 2E; $R^2 = 0.9947$; Kurtosis 0.6; Skewness 0.7).

By contrast, in the majority of CIE-withdrawn slices recorded, there was no significant change in the E_{50} at 60 min following tetanization, indicative of loss of E-S potentiation (Fig. 2E, n = 17 out of 21 slices; mean E_{50} difference: 0.3 ± 3.9 % from baseline; not significant from zero change at 60 min post-tetanus). Finally, when the tetanus trains were omitted in a separate group of naive and CIE-withdrawn slices, the peak of the E_{50} distribution showed no change in the E_{50} over the 60 min recording period in the majority of cases recorded (mean E_{50} difference in non-tetanized slices: Naive 0.1 ± 4.6% from baseline and CIE-withdrawn −3.3 ± 3.8 % from baseline; n = 12 slices each; not significant from zero change at 60 min in either group). Therefore, the data are consistent with significant suppression of E-S potentiation (i.e., E-S dissociation) with LTP in CIE-withdrawn slices.

E-S dissociation reflects indication of acute 24 hr withdrawal from CIE exposure

We next determined whether E-S potentiation loss by CIE exposure preceded the 24 h alcohol withdrawal period. Experiments were thus repeated in hippocampal slices prepared from a separate group of age-matched, early adolescent rats on their last CIE treatment day and before abstinence onset—henceforth designated as CIE non-withdrawn slices (see Methods). For these experiments, ethanol at concentrations similar to levels achieved *in vivo* (150 mg/dL) was maintained in the bath perfusate for the full duration of the recordings to prevent against potential withdrawal effects.

Similar to naïve hippocampal slices, CIE non-withdrawn slices largely exhibited a negative change in the E_{50} at 60 min following tetanization, indicative of E-S potentiation in the majority of cases recorded (n = 10 out of 16 slices, mean E_{50} difference: −20.3 ± 4.7 % from baseline, $p < 0.05$ versus zero change at 60 min post-tetanus by a one sample t-test; see also Fig. 6F, open columns). Between-group comparisons were made using the mean E_{50} value from the single E-S curve generated for each treatment group by averaging the pop. spike amplitudes and corresponding fEPSP slopes across incremental ranges. Results of this analysis indicated no significant difference in the mean E_{50} value at baseline, indicative of similar initial fEPSP-to-spike efficacies across all treatment groups (Fig. 2F, first set of columns). LTP induction by the 100 Hz tetanus stimulations resulted in significantly reduced mean E_{50} values (i.e., increased pop. spike efficacy) in both naïve and CIE non-withdrawn slices (Fig. 2F, $p < 0.001$ before versus after 100 Hz tetanus for each data set, with no significant difference between the two groups), whereas this LTP effect was absent in the case for the CIE-withdrawn slices recorded (Fig. 2F). Consequently, CIE-withdrawn slices as compared to naïve controls exhibited significantly diminished pop. spike efficacy following LTP induction (Fig. 2F; second set of columns; mean E_{50} value at 60 min post-tetanus: Naive 2.7 ± 0.1 mV/ms and CIE-withdrawn 3.6 ± 0.1 mV/ms; $p < 0.001$ Naive versus CIE-withdrawn).

Also examined was the question of whether E-S dissociation in CIE-withdrawn slices reflected an effect of CIE treatment on dendrosomatic conduction, which would result in diminished EPSP size at the CA1 soma. We measured the peak initial slope of the rising phase of the somatic fEPSP relative to the incoming excitatory input (i.e., somatic/dendritic fEPSP slope ratio) and found no effect of CIE withdrawal on this parameter at stimulus intensities near pop. spike threshold (somatic/dendritic fEPSP slope ratios: Ctr, 0.6 ± 0.1 and CIE-withdrawn 0.6 ± 0.1, n = 7 and 8 slices, respectively). Likewise, the fEPSP ratio was

unaffected by E-S potentiation in naïve slices that underwent tetanization (somatic/dendritic fEPSP ratio after tetanus 0.7 ± 0.1, not significantly different from before tetanus, n = 7 slices). Therefore, it is unlikely that E-S potentiation (Jester et al., 1995) or its loss by prior CIE exposure reflects altered EPSP conduction from dendrites to soma.

Sigma-1 receptor selective antagonist BD1047 reverses loss of E-S potentiation during acute alcohol abstinence

We uncovered previously a requirement for sigma-1 receptor function in the development of large amplitude LTP in CIE-withdrawn hippocampal slices (Sabeti and Gruol, 2008), whereas these receptors were shown to play no role in typical NMDA-receptor dependent LTP under normal conditions (Sabeti and Gruol, 2008; Sabeti et al., 2007). Sigma-1 receptors are expressed at both neuronal soma and dendritic inputs (Alonso et al., 2000) where they have been shown to either inhibit or activate a variety of voltage-dependent ion channels (Cheng et al., 2008; Martina et al., 2007; Zhang and Cuevas, 2002; Zhang and Cuevas, 2005) and, perhaps, affect neuronal excitability (Zhang and Cuevas, 2005, but see Cheng et al., 2008) depending on the nature of the activating ligand present. Therefore, we investigated whether sigma-1-receptor activation contributed to the E-S coupling abnormalities associated with large amplitude LTP in CIE-withdrawn slices.

Pharmacological blockade of endogenous sigma-1 receptors with bath-application of the selective antagonist BD1047 (Matsumoto et al., 1995; 1 uM, beginning at 30 min prior to LTP induction) resulted in partial or full restoration of E-S potentiation in individual CIE-withdrawn slices (Fig. 3A-B), with the peak of the E_{50} distribution indicating a significant leftward shift towards E-S potentiation at 60 min following tetanization in the majority of cases recorded (Fig. 3B; 13 out of 19 slices; mean E_{50} difference: −20.7 ± 3.6 % from baseline, $p < 0.001$ versus zero change from baseline at 60 min post-tetanus by a one sample t-test). On average, the pop. spike efficacy or mean E_{50} value was restored by BD1047 pretreatment in CIE-withdrawn slices to that expressed in naïve slices during LTP (Fig. 3C second set of columns). By contrast, in naïve slices, BD1047 pretreatment was without significant effect on either the E_{50} distribution (Fig. 3B versus Fig. 2E, mean E_{50} difference: +BD1047 −24.5 ± 6.1 % from baseline versus no BD1047 −18.4 ± 3.0 % from baseline; $p < 0.001$ versus zero change at 60 min post-tetanus by a one sample t-test for each set and no significant difference between sets) or the mean E_{50} value during LTP (Fig. 3C, open set of columns). Thus, BD1047 pretreatment prior to LTP induction restored the loss of E-S potentiation associated with adolescent CIE withdrawal, without affecting E-S plasticity in naïve control slices.

To endorse the involvement of sigma-1 receptor actions on E-S dissociation, we determined if effects of CIE withdrawal on E-S coupling could be reproduced in control slices by a sigma-1 receptor selective agonist added directly to the bath solution. For these studies, we first tested effects of the neuroactive steroid pregnenolone sulfate (PREG-S), a reported endogenous sigma-1 receptor agonist (Su et al., 1988) previously shown to enhance synaptic LTP responses in rat hippocampus (Chen et al., 2010; Sabeti et al., 2007). PREG-S bath application (5 μM; beginning at 30 min prior to LTP induction and for the remaining duration of the experiment) in ethanol-naive slices resulted in marked loss of E-S potentiation after LTP induction (Fig. 4A, n = 12 out of 19 slices; mean E_{50} difference: 7.8 ± 3.6 % from baseline; not significant from zero change at 60 min post-tetanus). Effects of PREG-S (5 μM) were occluded by co-application with BD1047 (1 μM), such that the E_{50} distribution was significantly shifted towards E-S potentiation with LTP in most cases (Fig. 4B, n = 8 out of 13 slices; mean E_{50} difference: −17.0 ± 5.5 % from baseline; $p < 0.05$ versus zero change at 60 min post-tetanus by a one sample t-test). By contrast, bath-application of 3α,5β sulfate, a structurally different sulfated neurosteroid analogue, did not impact E-S plasticity; ethanol-naive slices continued to exhibit E-S potentiation in the

presence of 3α,5β sulfate in the bath solution (5 μM; Fig. 4C, 8 out of 10 slices; mean E_{50} difference: −25.0 ± 4.0 % from baseline; $p < 0.05$ versus zero change at 60 min post-tetanus).

E-S dissociation reflects sigma-1 receptor modulatory actions on the somatic field EPSP time course

The data above suggested that sigma-1 receptors were functionally activated in CIE-withdrawn slices and participated in E-S dissociation during LTP. Repetitive stimulations are shown to trigger lasting modifications reflected in both the intracellularly and extracellularly recorded EPSP time course (Hess and Gustafsson, 1990; Taube and Schwartzkroin, 1988) in ways that alter synaptic integration/summation and spike generation (Fricker and Miles, 2000; Wang et al., 2003). In hippocampal pyramidal neurons, the intracellularly recorded EPSP time course is a critical variable in determining the consequence of synaptic activity on the spike output status (Fricker and Miles, 2000). Therefore, we evaluated the fEPSP decay time course to enable us to derive meaningful insights into the involvement of factors that shape the field EPSP and, perhaps, convey the sigma-1 receptor related effects on E-S potentiation. As part of our analysis, evoked fEPSP decay time constants were measured as a function of the observed differences in E-S potentiation between naive and CIE exposed animals using a subset of slices from data shown in Fig. 2E-F.

Results of such analyses indicated that LTP induction resulted in an overall slowing of the fEPSP time course at dendritic inputs, demonstrated as an increased decay tau value at 60 min post-tetanus relative to the baseline value in all slices recorded (Fig. 5A, overall significant effect of LTP on the tau value at dendrites: $F_{1, 54} = 12.2$, $p < 0.001$ before versus after LTP induction). No significant treatment group differences were evident prior to LTP induction in either the dendritic (Fig. 5A) or somatic (Fig. 5C) fEPSP decay time course at baseline (Fig. 5A and C, open columns).

By contrast at CA1 soma, where E-S coupling is believed to occur, a substantial slowing of the somatic fEPSP decay time course near threshold was evident but only in naïve slices that exhibited E-S potentiation (Fig. 5C, first set of columns, tau value at soma: before 4.5 ± 0.3 ms and after-LTP 6.8 ± 0.2 ms, $p < 0.001$ before versus after LTP). Such an effect of LTP was completely occluded in CIE-withdrawn slices that failed to become E-S potentiated (Fig. 5C, last set of columns). Thus, analyses of the fEPSP decay tau values indicated a significant LTP × CIE treatment interaction on the mean somatic fEPSP lifetime (Fig. 5C, $F_{2,54} = 4.5$, $p < 0.05$), resulting in a shortened somatic fEPSP duration during LTP in CIE-withdrawn as compared to naïve slices (Fig. 5C, first and last filled columns, tau value at 60 min post-tetanus: Naive 6.8 ± 0.2 ms and CIE-withdrawn 5.5 ± 0.4 ms, $p < 0.05$ Naive versus CIE-withdrawn).

Interestingly, similar to E-S potentiated naïve slices, CIE non-withdrawn slices that expressed E-S potentiation showed a noticeable trend towards a prolonged somatic fEPSP duration after LTP, as indicated by a ~23% increase in the decay tau value at 60 min post-tetanus, although the effect did not reach statistical significance (Fig. 5C, middle set of columns, tau value: before 5.7 ± 0.5 ms; after-LTP 7.0 ± 0.5 ms).

Decay tau values were also evaluated in BD1047 pretreated naïve and CIE-withdrawn slices from experiments shown in Fig. 3. Such analyses show that naïve slices were completely unresponsive to BD1047 pretreatment (1 μM) with respect to the LTP-induced changes in the dendritic (Fig. 5B, open columns) and somatic (Fig. 5D) fEPSP time course. By contrast BD1047 pretreatment in CIE-withdrawn slices facilitated the effect of LTP in prolonging the somatic fEPSP time course (Fig. 5D, tau value at 60 min post-tetanus: +BD1047 148.7 ±

11.6 % of baseline, n = 7 slices, $p < 0.05$ versus 100 % of baseline by a one sample t-test), whereas this effect was occluded in CIE-withdrawn slices not exposed to the antagonist (Fig. 5D, no BD1047 103.4 ± 6.6 % of baseline, n = 9 slices, not significant from 100 % or no change from baseline). Therefore, sigma-1 receptors acted in CIE withdrawn slices to shorten the somatic fEPSP decay time course during LTP.

E-S dissociation in acute alcohol abstinence is independent of NMDA receptor function

Dependency of E-S potentiation on NMDA receptor function was investigated using the NMDA receptor antagonist D-AP5 applied in the bath solution (50 μM; beginning at 30 min prior to LTP induction). As expected in naïve slices, the 100 Hz tetanus stimulations in the presence of dAP5 were completely unable to induce LTP in the fEPSP slope (Fig. 6A, 99.7 ± 4.6 % of baseline fEPSP slope, n = 7 slices at 60 min post-tetanus) or pop. spike amplitude (Fig. 6A). By comparison, in the absence of D-AP5 in the bath, the same tetanus stimulations in naïve slices resulted in potentiated fEPSP slope and pop. spike amplitudes consistent with LTP (Fig. 6A open and closed bars, respectively). D-AP5 bath-application also effectively blocked the induction of E-S potentiation in the majority of naïve slices recorded (Fig. 6B, closed bars; 9 out of 12 slices; mean E_{50} difference: −2.2 ± 5.0 % from baseline, not significant from zero change at 60 min post-tetanus), demonstrating a requirement of synaptic NMDA receptor function for both LTP and E-S potentiation under control conditions.

In the case for CIE-withdrawn slices, pharmacological blockade of NMDA receptors by inclusion of D-AP5 in the bath (50 μM) fully blocked LTP of the somatic pop. spike amplitude (Fig. 6C); however, there was no effect of D-AP5 on the CIE-induced loss of E-S potentiation (Fig. 6D; mean E_{50} difference: −2.0 ± 2.8 % from baseline, n = 18 slices; not significant from zero change at 60 min post-tetanus). Interestingly, and in agreement with our previous study (Sabeti and Gruol, 2008), LTP in the dendritically recorded fEPSP magnitude was not blocked by the presence of D-AP5 in the bath solution (Fig. 6C). Rather, a sustained LTP-like increase in the incoming dendritic fEPSP size was evident in CIE-withdrawn slices with D-AP5 present (Fig. 6C), reaching magnitudes that would normally trigger measurable pop. spike amplitudes in LTP-activated naive slices (for instance, see the E-S coupling curve after tetanus in Fig. 2C). Thus, D-AP5 pretreatment inhibited the pop. spike LTP response, despite the growing potentiation in the fEPSP magnitude (Fig. 6C), consistent with our finding above showing reduced pop. spike efficacy with LTP in CIE-withdrawn slices (Fig. 2F).

We also assessed NMDA receptor function in CIE non-withdrawn slices with respect to LTP and E-S potentiation. Bath application of D-AP5 (50 μM; beginning at 30 min prior to LTP induction) blocked LTP of the dendritic fEPSP slope and pop. spike amplitude in CIE non-withdrawn slices (Fig. 6E). E-S potentiation was also effectively blocked by D-AP5 pretreatment in the majority of CIE non-withdrawn slices recorded (Fig. 6F, closed bars; 5 out of 6 slices), similar to effects observed in naïve slices (Fig. 6B), providing evidence for intact NMDA receptor function in slices from CIE exposed non-withdrawn animals.

No apparent correspondence between E-S dissociation by alcohol and increased recurrent feedback inhibition

We considered if enhanced activation of feedback inhibitory inputs at CA1 soma contributed to the loss of E-S potentiation in CIE withdrawn slices. Paired-pulse stimulations were delivered to the CA3 afferent inputs at short 10 ms inter-pulse intervals to assess feedback inhibitory function, reflected as a decrease in the second relative to the first evoked pop. spike amplitude (Meyer et al., 1999).

For the first set of experiments, paired stimulations were delivered at the maximal test stimulus intensity and in the absence of a GABA-A receptor modulating agents to ensure full activation of CA1 inhibitory feedback circuits. Evoked inhibition was evaluated both before (baseline) and 60 min after LTP induction by the 100 Hz stimulations. Between slice comparisons of paired-pulse inhibition levels indicated significantly reduced evoked inhibition in CIE-withdrawn relative to naïve control slices over the two time points considered (Table 1, Baseline and 60 min post LTP, respectively: Naïve 77.6 ± 6.4% and 55.1 ± 7.7%, n = 15 slices; CIE-withdrawn 63.3 ± 5.6% and 39.1 ± 8.4%, n = 17 slices; main effect of CIE: $F_{1,60} = 4.5$, $p < 0.05$). However, LTP activation produced a similar percentage reduction in paired-pulse inhibition levels from baseline in both the naïve control and CIE-withdrawn slices recorded (Table 1, third column, mean percent decrease in paired-pulse inhibition levels: Naïve −32.7 ± 6.8% and CIE-withdrawn: −44.3 ± 9.6% from baseline, n = 15 and 17, respectively at 60 min post tetanus, $p < 0.001$ versus zero change for each group by a one-sample t-test and no significant difference between groups). Evoked inhibition was also compared in naive slices that expressed E-S potentiation and CIE-withdrawn slices that failed to become E-S potentiated (i.e., data from the peaks of the E_{50} distributions in Fig. 2E) and no significant difference between slices was observed in the effect of LTP in reducing paired-pulse inhibition (Fig. 7A, mean decrease in paired-pulse inhibition levels: Naïve, E-S potentiated −41.3 ± 7.6 % from baseline and CIE-withdrawn, non E-S potentiated −47.3 ± 12.3 % from baseline, n = 11 slices each at 60 min post-tetanus, $p < 0.001$ versus zero change from baseline for each group by a one sample t-test).

At the near half-maximal stimulation intensity, there was no main effect of CIE withdrawal on paired-pulse inhibition levels over the two time points considered (Table 1) and, again, the mean percentage decrease in paired pulse inhibition by LTP was similar between naïve and CIE-withdrawn slices (Table 1; Fig. 7D, first set of columns, $p < 0.01$ versus zero change from baseline for Naive and CIE-withdrawn, n = 8 and 7 slices at 60 min post-tetanus, respectively). Thus, the strong recurrent feedback inhibition at baseline was generally overcome by LTP, but this effect did not always account for the differential propensity of naïve and CIE-withdrawn slices in exhibiting E-S potentiation.

We next determined whether variations existed in the NMDA receptor contribution to feedback inhibition plasticity in naïve versus CIE-withdrawn slices. Results indicated that D-AP5 pretreatment (50 μM; beginning at 30 min prior to LTP induction) occluded the effect of LTP in reducing paired-pulse inhibition at the maximal stimulus intensity tested in both naïve and CIE-withdrawn slices (Table 1, Fig 7B and C, third columns). As well, neither naïve nor CIE-withdrawn slices showed significant change in paired-pulse inhibition levels over a 60 min recording period when the tetanus trains were omitted (Table 1, Fig. 7B and C, open columns). Therefore, paired-pulse inhibition was overcome by LTP via a mechanism that required synaptic activation and intact NMDA receptor function in the case for both naïve and CIE-withdrawn slices.

We also evaluated effects of D-AP5 (50 μM) application per se on evoked inhibition and found no significant change in paired-pulse inhibition levels over a 30 min drug perfusion period in non-tetanized naïve or CIE-withdrawn slices (change in paired-pulse inhibition: Naive −3.6 ± 5.7% from baseline and CIE-withdrawn +4.0 ± 3.5 % from baseline, n = 8 and 12 slices, respectively, not significant versus zero change at 30 min by a one sample t-test). These last results rule out a major contribution of NMDA receptors on GABA interneurons in eliciting recurrent feedback inhibition and, rather, point to NMDA receptor actions, presumably originating at CA3-CA1 excitatory synapses, in the effects of LTP in reducing feedback inhibition.

Paired-pulse inhibition in presence of 3α,5β sulfate, a negative modulator of GABA-A receptors—Paired-pulse inhibition is based predominately on activity of GABA-A receptors on CA1 postsynaptic neurons (Meyer et al., 1999; Steffensen and Henriksen, 1991; Thomas et al., 2005); however, other factors including presynaptic depletion and/or Na^+ channel inactivation, for instance, may have differentially contributed to evoked inhibition in CIE-withdrawn slices. To preliminarily address this issue, paired-pulse inhibition was compared between naïve and CIE-withdrawn slices by (1) using a lower, near half-maximal stimulus voltage expected to promote presynaptic deletion or Na^+ channel inactivation to a lesser degree (Zucker and Regehr, 2002) and (2) assessing evoked inhibition in the presence of the neurosteroid 3α,5β sulfate, a known negative modulator of GABA-A receptor activity (Mennerick et al., 2008; Wang et al., 2002) with demonstrated efficacy in inhibiting GABA-A receptor mediated responses in hippocampus (Park-Chung et al., 1999).

Bath application of 3α,5β sulfate (5 μM; 30 min prior to LTP induction with continuous perfusion throughout) near-completely abolished the effect of LTP in reducing paired-pulse inhibition at near half maximal stimulation strengths in naive slices, with no significant decrease in evoked inhibition levels after versus before LTP induction (Table 1, Fig. 7D, open columns, mean decrease in inhibition: Naive −8.4 ± 13.4% from baseline, n = 7 slices each at 60 min post-tetanus, not significant versus zero change from baseline). Interestingly, the maximal stimulation intensity applied overcame the effect of 3α,5β sulfate; and naïve slices continued to show robust reductions in evoked inhibition levels after LTP even with the neurosteroid present in the bath solution (Table 1, Fig. 7E, open columns). These results demonstrate both an underlying 3α5β-sulfate-sensitive and, presumably, GABA-A receptor mediated component of reduced feedback inhibition by LTP, as well as a 3α,5β sulfate-insensitive component that is recruited at the higher stimulation intensities applied.

By contrast to the case for naïve slices, CIE-withdrawn slices pretreated with 3α5β-sulfate in the bath solution (5 μM) showed an overall increase in paired-pulse inhibition levels, with a significant main effect of CIE treatment on evoked inhibition levels at the near half-maximal stimulation intensities tested (Table 1, $F_{1,24} = 7.7$; $p < 0.05$ versus naïve pretreated slices). Likewise, CIE-withdrawn slices achieved significantly greater paired-pulse inhibition levels in the presence versus absence of 3α,5β sulfate at both the maximal and near half-maximal stimulation intensities tested (Table 1, $p < 0.05$ 3α,5β sulfate versus ACSF at 60 min post tetanus). Within slice comparisons of the mean percentage change in evoked inhibition levels at the maximal stimulation strength indicated a trend, albeit insignificant, towards a greater protection afforded against the effect of LTP in reducing recurrent inhibition in CIE-withdrawn versus naïve slices with 3α5β sulfate present (Table 1, Fig. 7E, second set of columns, mean decrease in inhibition with 3α,5β sulfate present: Naive −46.5 ± 11 % from baseline and CIE withdrawn −26.8 ± 5.3 % from baseline, n = 9 and 7 slices, respectively at 60 min post-tetanus, $p < 0.01$ versus zero change for each group by a one sample t-test and no significant difference between groups).

Antagonist BD1047 is without effect on plasticity of feedback inhibition

Results above suggested that altered plasticity of feedback inhibition was insufficient to account for E-S dissociation in CIE-withdrawn slices; therefore, we confirmed in additional experiments if the sigma-1 receptor antagonist BD1047 restored E-S potentiation via actions independent of plasticity at inhibitory feedback circuits. For these experiments, effects of BD1047 bath-application on paired-pulse (10 ms) inhibition were investigated using the maximally applied test stimulus voltage—the intensity suggested above to recruit both the 3α,5β sulfate-sensitive and -insensitive components of evoked inhibition (Fig. 7D-E). Results show that BD1047 (1 μM) application over a 30 min perfusion period was without

significant effect on baseline paired-pulse inhibition levels in non-tetanized slices (change in paired-pulse inhibition at 30 min after BD1047 application: Naive +1.2 ± 5.1 % from baseline and CIE-withdrawn +1.2 ± 5.0 % from baseline, n = 9 and 10 slices, respectively, not significant versus zero change in either group by a one sample t-test). Moreover, LTP induction effectively reduced paired-pulse inhibition, and to a similar extent, in both naïve and CIE-withdrawn slices pretreated with BD1047 (Table 1, Fig. 7B and 7C, respectively, slashed columns), similar to effects observed in the absence of BD1047 in the bath solution (Table 1, Fig. 7B-C, closed versus slashed columns).

Discussion

Although activity-induced changes in synaptic strength (LTP) are long recognized to underlie modifications in neural circuits essential for learning and memory, evidence suggests that the intrinsic excitability of neurons in both the developing (Turrigiano and Nelson, 2004) and mature brain (Daoudal and Debanne, 2003; Zhang and Linden, 2003) is also dynamically modulated in response to experience. For instance, experience-induced increases in CA1/CA3 neuronal excitability, indexed by EPSP-to-spike (E-S) potentiation (Daoudal et al., 2002) and/or reduced post-burst afterhyperpolarization, are reported during hippocampal driven conditioned responses (Brown and Randall, 2009; McKay et al., 2009; Moyer et al., 1996), thus favoring a role for intrinsic neuronal plasticity in associative learning and memory.

Findings here newly demonstrate that, while LTP-like potentiation exists at CA1 dendritic synapses in early adolescent CIE withdrawn animals, the input-output curve of neurons is markedly shifted towards inhibited E-S potentiation in the CA1 region. Impaired E-S potentiation with LTP reflects increased activity of sigma-1 receptors, resulting in a shortened somatic field EPSP duration and E-S dissociation in CIE withdrawn hippocampal slices. A sigma-1 receptor selective antagonist BD1047 is shown here to effectively reverse the E-S coupling abnormalities in CIE withdrawn slices and restore synaptic LTP amplitudes to normal levels as previously demonstrated (Sabeti and Gruol, 2008). Sigma-1 receptor mediated abnormalities in E-S plasticity appear independent of changes in NMDA- or GABA-receptor related neuroplastic processes and, therefore, likely involve the aid of voltage-dependent ion channel(s) that are known to shape the EPSP time course and, thereby, alter the spike output status. Such findings highlight a novel mechanism involving ongoing sigma-1 receptor activation through which alcohol can impact hippocampal functioning by means other than reducing LTP magnitudes.

Intermittent alcohol vapor exposure and relevance of acute alcohol abstinence effects

The present study assessed various indices of excitatory synaptic function and plasticity in hippocampus at 24 hr into withdrawal from intermittent ethanol vapor exposure. Many groups have employed the alcohol vapor exposure procedure for cultivating symptoms of alcohol dependence in animal models because of its predictive validity in demonstrating medication effectiveness in altering drinking behavior (O'Dell et al., 2004; Rimondini et al., 2002). Alcohol vapor exposure at intoxicating blood alcohol concentrations similar to those achieved here is shown to be efficacious in increasing voluntary alcohol consumption and withdrawal-induced anxiety behaviors when exposure occurs over at least a 2-week period (O'Dell et al., 2004; Sommer et al., 2008).

Repeated cycles of intoxication and abstinence tend to exacerbate alcohol-dependence symptoms (O'Dell et al., 2004), but not due to any adverse health consequences of ethanol vapor exposure per se (Di Luzio and Stege, 1979; Rimondini et al., 2002) or to non-specific environment-induced stress effects (Lee et al., 2000), which are reportedly very minimal if not nonexistent. The rising and falling pattern of high blood alcohol levels produced by the

intermittent alcohol vapor exposure follow that reported in alcohol-dependent animals on a liquid alcohol diet (Gilpin et al., 2009), suggesting that oscillating patterns of high alcohol intake, rather than route of alcohol administration, are a common underlying factor in triggering neuroadaptations mediating addiction progression.

Findings here reveal prominent E-S dissociation and reduced spike efficacy of CA1 excitatory neurons during synaptic activity and in the state of acute (24 hr) abstinence from alcohol. The persistence of E-S dissociation and related phenotypes at protracted periods of abstinence remains to be investigated. However, with more prolonged abstinence periods, evidence supports a withdrawal-induced neuronal hyperexcitability reflecting increased glutamatergic activity within hippocampal and limbic-cortical systems that mediate emotional regulation (Hendricson et al., 2007). Thus, increased neuronal excitability may contribute to the emergence of a negative affective state described in the late clinical stages of addiction (Spanagel, 2009). Hippocampal CA1 neurons provide the main excitatory output connections to accumbal and amygdalar nuclei within limbic-cortical circuitry. It is possible that alterations in intrinsic CA1 excitability at the 24 hr time point of alcohol withdrawal investigated here represent a signaling trigger for more enduring changes in circuit function (Hendricson et al., 2007). Regardless, the appearance of a progressive sequence of negative affective symptomatology in the chronic alcohol vapor exposed model (Sommer et al., 2008), including increasing neurocognitive dysfunction within several days after cessation of alcohol administration (Slawecki et al., 2004), would indicate that the early time points of abstinence may be an important target of pharmacological intervention in addictive disease progression.

Inhibition of E-S plasticity following intermittent ethanol exposure in early-adolescence

Activity induced increase in intrinsic neuronal excitability has been demonstrated previously in hippocampus in the form of induced modifications in the E-S coupling properties of neurons, resulting in an increased number of action potential spikes at any given level of synaptic drive (Abraham et al., 1987; Andersen et al., 1980; Taube and Schwartzkroin, 1988). Consistent with increased neuronal excitability during LTP, we find naïve control slices display a robust leftward shift in the input-output pattern of evoked population responses towards E-S potentiation, which is accompanied by a longer lasting field EPSP at the CA1 soma. By contrast, inhibited E-S potentiation in CIE-withdrawn slices is associated with significantly shortened field EPSP duration at CA1 soma than would be anticipated at LTP activated pathways. Findings here are, therefore, consistent with intracellular studies in hippocampal pyramidal neurons where it is reasonably clear that the spike output is guided by intrinsic neuronal factors that shape the EPSP time course and, thereby, alter synaptic integration (Fricker and Miles, 2000). For example, a prolonged EPSP time course would presumably facilitate the spatial/temporal summation of inputs on a pyramidal neuron (Wang et al., 2003) resulting in increased neuronal excitability with LTP (Campanac et al., 2008); whereas a shortened EPSP duration induced by large amplitude LTP responses above an optimal level decrease intrinsic excitability (Fan et al., 2005). Thus, effects of acute alcohol abstinence on E-S plasticity appear to impinge on the same plasticity machinery by which CA1 neurons dynamically regulate their action potential output based on changing levels of synaptic excitation.

A number of elegant studies demonstrate an up-regulation of NMDA receptor expression resulting in synaptic dysfunction following chronic alcohol exposure (Carpenter-Hyland and Chandler, 2007). Effects of chronic alcohol on the expression of NMDA receptor subtypes are also highly age-dependent (Pian et al., 2010) and appear to play a role in developmental differences between adolescent and adult rats in their LTP and memory responding to alcohol (Pyapali et al., 1999; Sabeti and Gruol, 2008; White and Swartzwelder, 2005). The present study did not directly assess effects of CIE exposure on isolated NMDA receptor

mediated responses, which may have contributed to postsynaptic E-S dissociation. However, if increased basal NMDA-receptor activity were the main contributor to E-S dissociation, we would expect recovery of E-S potentiation by D-AP5 pretreatment. Yet, we found no response to D-AP5 (50 μM) in CIE-withdrawn slices and speculate that the alcohol-induced change in E-S coupling appears independent of the expression of NMDA receptor plasticity induced by chronic alcohol exposure.

The present findings show no apparent correspondence between increased levels of recurrent inhibition and E-S dissociation with LTP. First, LTP activation is shown to generally overcome strong recurrent inhibition in both naïve and CIE-withdrawn hippocampal slices, regardless of the E-S coupling phenotype exhibited with LTP. Second, the neurosteroid 3α, 5β sulfate occludes the effects of LTP on recurrent inhibition at sub-maximal stimulation intensities tested in naïve control slices, as would be expected with a GABA-A receptor negative modulator. However, this effect of 3α,5β sulfate is of no significant consequence to the outcome of LTP on E-S potentiation in naïve slices (Fig. 4C). Finally, 3α,5β sulfate bath application unmasks a significantly greater level of paired-pulse inhibition in CIE-withdrawn versus naïve slices, suggestive of triggering in the former a non-specific response to 3α,5β sulfate (Liu et al., 2002;Malayev et al., 2002). Alternatively, results here with 3α,5β sulfate would suggest a potential interplay among both GABA-A receptor mediated (e.g., altered GABA receptor density or kinetics) and non GABA-A receptor mediated (e.g., desensitized Na^+ channels) mechanisms underlying E-S dissociation by alcohol. The present experiments do not provide information on the steady state inhibition or potential role of faster feedforward inhibitory processes to E-S dissociation, which merit further intracellular characterization.

Previously we found that the transition from early-to-late stage adolescence is a critical period determining the exact outcome of alcohol exposure on synaptic LTP measures: thus, late adolescent animals resemble adult rats in showing decreases in synaptic LTP levels following chronic alcohol exposure (Sabeti and Gruol, 2008), while early-adolescent rats exhibit an increase in LTP (Sabeti and Gruol, 2008) and accompanying E-S dissociation as seen here. It would be valuable to know if chronic alcohol administration in adulthood produces similar effects on hippocampal E-S coupling function; however, we hypothesize that such would not be the case because rats with a history of chronic alcohol vapor exposure as post-pubescent adults do not achieve the large amplitude LTP responses reportedly needed to trigger E-S dissociation (Campanac et al., 2008). Because early adolescent as compared to adult rats appear to show more enduring alterations in NMDA subunit receptor expression several weeks into alcohol abstinence (Pian et al., 2010), a finer assessment of enduring alterations in hippocampal function by adolescent alcohol exposure is critically warranted.

Sigma-1 receptor selective antagonist BD1047 effective against alcohol-withdrawal induced E-S dissociation

Findings here advance evidence for the functional activation of hippocampal sigma-1 receptors by chronic alcohol exposure in early adolescence: the sigma-1 receptor antagonist BD1047, on its own, restores E-S potentiation in CIE-withdrawn slices but is without effect on E-S plasticity parameters in LTP-activated naive slices. While a single concentration of BD1047 was tested here, pharmacological characterizations in rat brain support its high affinity binding to sigma-1 receptors, in contrast to its negligible affinity at other sites, including NMDA, opioid, dopamine D_2, $5HT_1$ and muscarinic acetylcholine receptors (Matsumoto et al., 1995). The 24 hr withdrawal period from alcohol appears to be critical for the development of sigma-1 receptor mediated E-S dissociation because hippocampal slices from CIE non-withdrawn animals retain several plasticity characteristics, including NMDA-receptor dependent LTP and increased likelihood of E-S potentiation. Our finding

that the 100 Hz stimulation trains effectively trigger E-S potentiation in CIE non-withdrawn slices further rule out effects of the tetanus stimulations per se on altered sigma-1 receptor function.

The basis for the functional induction of sigma-1 receptors following acute withdrawal from early adolescent CIE treatment remains to be investigated; however, several studies suggest the possibility for upregulation in mRNA and/or protein levels of sigma-1 receptors following exposure to abused drugs (Liu and Matsumoto, 2008; Stefanski et al., 2004). Another possibility is an increase in brain concentrations of endogenous sigma-1 receptor agonists, including one or several neurosteroids induced by alcohol actions (VanDoren et al., 2000). In support of the latter hypothesis, our findings and those others illustrate that increasing concentrations of certain neurosteroid agonists at sigma-1 receptors facilitate LTP formation at hippocampal synapses (Chen et al., 2010; Chen et al., 2006; Sabeti et al., 2007) and block E-S potentiation in otherwise healthy naïve slices (Fig. 4A), thus appearing to mimic CIE withdrawal effects on both synaptic LTP and E-S plasticity. Remaining to be investigated is whether the appearance of BD1047 drug effects on E-S coupling may reflect altered protein-protein interactions, for instance, those that promote sigma-1 receptor trafficking to the plasma membrane (Hayashi et al., 2000) and/or enhance sigma-1 receptor affinity for their endogenous non-steroid ligand(s) (Fontanilla et al., 2009).

We demonstrated previously that the induction of sigma-1 receptors results in transiently increased glutamate release probability during brief repetitive stimulations of CA3 afferent fibers in hippocampal slices (Sabeti et al., 2007). Short-lived presynaptic actions involving sigma-1 receptors also appear to contribute in part to the induction of large amplitude LTP responses during adolescent CIE withdrawal (Sabeti and Gruol, 2008). Building on these findings, results here reveal additional postsynaptic actions downstream of LTP induction and, thus, raise an intriguing possibility for a unique modulatory role of sigma-1 receptors in presynaptic-postsynaptic coordination, which may guide certain forms of experience-driven plasticity and learning (Dan and Poo, 2006). Future investigations are warranted to test this possibility in detail.

Potential molecular mechanisms and functional implications

The present findings reveal selective effects of BD1047 on the field EPSP time course predominately at CA1 soma, as opposed to dendritic input sites. Furthermore, at the CA1 soma, sigma-1 receptor mediated actions appear to have a discriminating effect on the EPSP decay time course but not initial fEPSP slope. Regional variations exist in the density and subtypes of ion channels along the somatodendritic axis of CA1 pyramidal neurons (Spruston, 2008), which may contribute to differential EPSP shape/efficacy and, potentially, account for the restricted actions of BD1047 at CA1 soma. For instance, a possible explanation of the data would be sigma-1 receptor modulatory actions on select voltage-sensitive conductance(s) that regulate fEPSP decay but are not activated early enough to control the rising phase of the fEPSP. The goal of future intracellular investigations will be to identify the exact voltage-gated ion channels underlying the E-S plasticity defects associated with adolescent CIE withdrawal. Likely candidates include voltage-gated Na^+ and A-type K^+ ion-channels that are reported targets of sigma-1 receptor actions (Aydar et al., 2002; Cheng et al., 2008; Martina et al., 2007; Zhang and Cuevas, 2005) and also implicated in intrinsic neuronal plasticity regulation (Frick et al., 2004; Jung and Hoffman, 2009; Xu et al., 2005). For example, negative regulation of voltage-dependent Na^+ channels by sigma-1 receptors (Cheng et al., 2008) would be consistent with an activity-dependent decrease in CA1 neuronal excitability related to depressed Na^+ channel function (Xu et al., 2005).

While the extracellular field recordings here did not allow a complete elucidation of the firing phenotype of individual CIE-withdrawn neurons, they effectively captured a decreased likelihood of E-S potentiation in the activated hippocampal network—effects which might be obscured with intracellular recordings from individual cells (Kaczorowski et al., 2007). The present findings, therefore, provide key analysis highlighting E-S plasticity in hippocampus as an important substrate for early withdrawal-induced alcohol actions on network behavior and, perhaps, a basis for altered memory processing that is not necessarily accounted for by changes in synaptic strength alone.

Acknowledgments

This study was supported by the K99 and R00 Pathway to Independence Award (AA01682) and the Alcohol Research Center grant (AA06420) from The National Institute on Alcohol Abuse and Alcoholism. We are grateful to Dr. Donna L. Gruol for helpful discussion and extend our thanks also to Maury Cole, Antonio Sweeney and Tess Kimber for expert operation of the ethanol vapor chambers.

Grant sponsor: NIH/NIAAA; *Grant numbers:* K99/R00-AA01682 and AA06420

References

Abraham WC, Gustafsson B, Wigstrom H. Long-term potentiation involves enhanced synaptic excitation relative to synaptic inhibition in guinea-pig hippocampus. J Physiol. 1987; 394:367–80. [PubMed: 3443970]

Alonso G, Phan V, Guillemain I, Saunier M, Legrand A, Anoal M, Maurice T. Immunocytochemical localization of the sigma(1) receptor in the adult rat central nervous system. Neuroscience. 2000; 97(1):155–70. [PubMed: 10771347]

Andersen P, Sundberg SH, Sveen O, Swann JW, Wigstrom H. Possible mechanisms for long-lasting potentiation of synaptic transmission in hippocampal slices from guinea-pigs. J Physiol. 1980; 302:463–82. [PubMed: 7411464]

Aydar E, Palmer CP, Klyachko VA, Jackson MB. The sigma receptor as a ligand-regulated auxiliary potassium channel subunit. Neuron. 2002; 34(3):399–410. [PubMed: 11988171]

Brown JT, Randall AD. Activity-dependent depression of the spike after-depolarization generates long-lasting intrinsic plasticity in hippocampal CA3 pyramidal neurons. J Physiol. 2009; 587(Pt 6): 1265–81. [PubMed: 19171653]

Brown SA, Tapert SF, Granholm E, Delis DC. Neurocognitive functioning of adolescents: effects of protracted alcohol use. Alcoholism, clinical and experimental research. 2000; 24(2):164–71.

Campanac E, Daoudal G, Ankri N, Debanne D. Downregulation of dendritic I(h) in CA1 pyramidal neurons after LTP. J Neurosci. 2008; 28(34):8635–43. [PubMed: 18716222]

Carpenter-Hyland EP, Chandler LJ. Adaptive plasticity of NMDA receptors and dendritic spines: implications for enhanced vulnerability of the adolescent brain to alcohol addiction. Pharmacology, biochemistry, and behavior. 2007; 86(2):200–8.

Chavez-Noriega LE, Bliss TV, Halliwell JV. The EPSP-spike (E-S) component of long-term potentiation in the rat hippocampal slice is modulated by GABAergic but not cholinergic mechanisms. Neurosci Lett. 1989; 104(1-2):58–64. [PubMed: 2554222]

Chen L, Cai W, Zhou R, Furuya K, Sokabe M. Modulatory metaplasticity induced by pregnenolone sulfate in the rat hippocampus: a leftward shift in LTP/LTD-frequency curve. Hippocampus. 2010; 20(4):499–512. [PubMed: 19475651]

Chen L, Dai XN, Sokabe M. Chronic administration of dehydroepiandrosterone sulfate (DHEAS) primes for facilitated induction of long-term potentiation via sigma 1 (sigma1) receptor: optical imaging study in rat hippocampal slices. Neuropharmacology. 2006; 50(3):380–92. [PubMed: 16364377]

Cheng ZX, Lan DM, Wu PY, Zhu YH, Dong Y, Ma L, Zheng P. Neurosteroid dehydroepiandrosterone sulphate inhibits persistent sodium currents in rat medial prefrontal cortex via activation of sigma-1 receptors. Exp Neurol. 2008; 210(1):128–36. [PubMed: 18035354]

Dan Y, Poo MM. Spike timing-dependent plasticity: from synapse to perception. Physiol Rev. 2006; 86(3):1033–48. [PubMed: 16816145]

Daoudal G, Debanne D. Long-term plasticity of intrinsic excitability: learning rules and mechanisms. Learn Mem. 2003; 10(6):456–65. [PubMed: 14657257]

Daoudal G, Hanada Y, Debanne D. Bidirectional plasticity of excitatory postsynaptic potential (EPSP)-spike coupling in CA1 hippocampal pyramidal neurons. Proc Natl Acad Sci U S A. 2002; 99(22):14512–7. [PubMed: 12391303]

Di Luzio NR, Stege TE. Influence of chronic ethanol vapor inhalation on hepatic parenchymal and Kupffer cell function. Alcohol Clin Exp Res. 1979; 3(3):240–7. [PubMed: 384834]

Durand D, Carlen PL. Impairment of long-term potentiation in rat hippocampus following chronic ethanol treatment. Brain Res. 1984; 308(2):325–32. [PubMed: 6541071]

Fan Y, Fricker D, Brager DH, Chen X, Lu HC, Chitwood RA, Johnston D. Activity-dependent decrease of excitability in rat hippocampal neurons through increases in I(h). Nat Neurosci. 2005; 8(11):1542–51. [PubMed: 16234810]

Fontanilla D, Johannessen M, Hajipour AR, Cozzi NV, Jackson MB, Ruoho AE. The hallucinogen N,N-dimethyltryptamine (DMT) is an endogenous sigma-1 receptor regulator. Science (New York, N Y). 2009; 323(5916):934–7.

Frick A, Magee J, Johnston D. LTP is accompanied by an enhanced local excitability of pyramidal neuron dendrites. Nature neuroscience. 2004; 7(2):126–35.

Fricker D, Miles R. EPSP amplification and the precision of spike timing in hippocampal neurons. Neuron. 2000; 28(2):559–69. [PubMed: 11144364]

Gilpin NW, Smith AD, Cole M, Weiss F, Koob GF, Richardson HN. Operant behavior and alcohol levels in blood and brain of alcohol-dependent rats. Alcohol Clin Exp Res. 2009; 33(12):2113–23. [PubMed: 19740131]

Hayashi T, Maurice T, Su TP. Ca(2+) signaling via sigma(1)-receptors: novel regulatory mechanism affecting intracellular Ca(2+) concentration. J Pharmacol Exp Ther. 2000; 293(3):788–98. [PubMed: 10869377]

Hayashi T, Su TP. Regulating ankyrin dynamics: Roles of sigma-1 receptors. Proc Natl Acad Sci U S A. 2001; 98(2):491–6. [PubMed: 11149946]

Hendricson AW, Maldve RE, Salinas AG, Theile JW, Zhang TA, Diaz LM, Morrisett RA. Aberrant synaptic activation of N-methyl-D-aspartate receptors underlies ethanol withdrawal hyperexcitability. J Pharmacol Exp Ther. 2007; 321(1):60–72. [PubMed: 17229881]

Hess G, Gustafsson B. Changes in field excitatory postsynaptic potential shape induced by tetanization in the CA1 region of the guinea-pig hippocampal slice. Neuroscience. 1990; 37(1):61–9. [PubMed: 1978743]

Jester JM, Campbell LW, Sejnowski TJ. Associative EPSP--spike potentiation induced by pairing orthodromic and antidromic stimulation in rat hippocampal slices. J Physiol. 1995; 484(Pt 3):689–705. [PubMed: 7623285]

Jung SC, Hoffman DA. Biphasic somatic A-type K channel downregulation mediates intrinsic plasticity in hippocampal CA1 pyramidal neurons. PLoS One. 2009; 4(8):e6549. [PubMed: 19662093]

Kaczorowski CC, Disterhoft J, Spruston N. Stability and plasticity of intrinsic membrane properties in hippocampal CA1 pyramidal neurons: effects of internal anions. J Physiol. 2007; 578(Pt 3):799–818. [PubMed: 17138601]

Land C, Spear NE. Ethanol impairs memory of a simple discrimination in adolescent rats at doses that leave adult memory unaffected. Neurobiology of learning and memory. 2004; 81(1):75–81. [PubMed: 14670361]

Lee S, Schmidt D, Tilders F, Cole M, Smith A, Rivier C. Prolonged exposure to intermittent alcohol vapors blunts hypothalamic responsiveness to immune and non-immune signals. Alcohol Clin Exp Res. 2000; 24(1):110–22. [PubMed: 10656200]

Lisman J. The theta/gamma discrete phase code occuring during the hippocampal phase precession may be a more general brain coding scheme. Hippocampus. 2005; 15(7):913–22. [PubMed: 16161035]

Liu QY, Chang YH, Schaffner AE, Smith SV, Barker JL. Allopregnanolone activates GABA(A) receptor/Cl(−) channels in a multiphasic manner in embryonic rat hippocampal neurons. J Neurophysiol. 2002; 88(3):1147–58. [PubMed: 12205136]

Liu Y, Matsumoto RR. Alterations in fos-related antigen 2 and sigma1 receptor gene and protein expression are associated with the development of cocaine-induced behavioral sensitization: time course and regional distribution studies. J Pharmacol Exp Ther. 2008; 327(1):187–95. [PubMed: 18591217]

Malayev A, Gibbs TT, Farb DH. Inhibition of the NMDA response by pregnenolone sulphate reveals subtype selective modulation of NMDA receptors by sulphated steroids. Br J Pharmacol. 2002; 135(4):901–9. [PubMed: 11861317]

Martina M, Turcotte ME, Halman S, Bergeron R. The sigma-1 receptor modulates NMDA receptor synaptic transmission and plasticity via SK channels in rat hippocampus. J Physiol. 2007; 578(Pt 1):143–57. [PubMed: 17068104]

Matsumoto RR, Bowen WD, Tom MA, Vo VN, Truong DD, De Costa BR. Characterization of two novel sigma receptor ligands: antidystonic effects in rats suggest sigma receptor antagonism. Eur J Pharmacol. 1995; 280(3):301–10. [PubMed: 8566098]

Maurice T, Casalino M, Lacroix M, Romieu P. Involvement of the sigma 1 receptor in the motivational effects of ethanol in mice. Pharmacol Biochem Behav. 2003; 74(4):869–76. [PubMed: 12667901]

Maurice T, Su TP. The pharmacology of sigma-1 receptors. Pharmacol Ther. 2009; 124(2):195–206. [PubMed: 19619582]

McKay BM, Matthews EA, Oliveira FA, Disterhoft JF. Intrinsic neuronal excitability is reversibly altered by a single experience in fear conditioning. J Neurophysiol. 2009; 102(5):2763–70. [PubMed: 19726729]

Mennerick S, Lamberta M, Shu HJ, Hogins J, Wang C, Covey DF, Eisenman LN, Zorumski CF. Effects on membrane capacitance of steroids with antagonist properties at GABAA receptors. Biophys J. 2008; 95(1):176–85. [PubMed: 18339741]

Meunier J, Demeilliers B, Celerier A, Maurice T. Compensatory effect by sigma1 (sigma1) receptor stimulation during alcohol withdrawal in mice performing an object recognition task. Behav Brain Res. 2006; 166(1):166–76. [PubMed: 16191445]

Meyer JH, Lee S, Wittenberg GF, Randall RD, Gruol DL. Neurosteroid regulation of inhibitory synaptic transmission in the rat hippocampus in vitro. Neuroscience. 1999; 90(4):1177–83. [PubMed: 10338288]

Morrisett RA, Swartzwelder HS. Attenuation of hippocampal long-term potentiation by ethanol: a patch-clamp analysis of glutamatergic and GABAergic mechanisms. J Neurosci. 1993; 13(5): 2264–72. [PubMed: 8478698]

Moyer JR Jr. Thompson LT, Disterhoft JF. Trace eyeblink conditioning increases CA1 excitability in a transient and learning-specific manner. J Neurosci. 1996; 16(17):5536–46. [PubMed: 8757265]

Nelson TE, Ur CL, Gruol DL. Chronic intermittent ethanol exposure enhances NMDA-receptor-mediated synaptic responses and NMDA receptor expression in hippocampal CA1 region. Brain Res. 2005; 1048(1-2):69–79. [PubMed: 15919065]

O'Dell LE, Roberts AJ, Smith RT, Koob GF. Enhanced alcohol self-administration after intermittent versus continuous alcohol vapor exposure. Alcohol Clin Exp Res. 2004; 28(11):1676–82. [PubMed: 15547454]

Park-Chung M, Malayev A, Purdy RH, Gibbs TT, Farb DH. Sulfated and unsulfated steroids modulate gamma-aminobutyric acidA receptor function through distinct sites. Brain Res. 1999; 830(1):72–87. [PubMed: 10350561]

Pian JP, Criado JR, Milner R, Ehlers CL. N-methyl-D-aspartate receptor subunit expression in adult and adolescent brain following chronic ethanol exposure. Neuroscience. 2010; 170(2):645–54. [PubMed: 20603193]

Pyapali GK, Turner DA, Wilson WA, Swartzwelder HS. Age and dose-dependent effects of ethanol on the induction of hippocampal long-term potentiation. Alcohol. 1999; 19(2):107–11. [PubMed: 10548153]

Rimondini R, Arlinde C, Sommer W, Heilig M. Long-lasting increase in voluntary ethanol consumption and transcriptional regulation in the rat brain after intermittent exposure to alcohol. FASEB J. 2002; 16(1):27–35. [PubMed: 11772933]

Roberto M, Nelson TE, Ur CL, Gruol DL. Long-term potentiation in the rat hippocampus is reversibly depressed by chronic intermittent ethanol exposure. J Neurophysiol. 2002; 87(5):2385–97. [PubMed: 11976376]

Sabeti J, Gruol DL. Emergence of NMDAR-independent long-term potentiation at hippocampal CA1 synapses following early adolescent exposure to chronic intermittent ethanol: role for sigma-receptors. Hippocampus. 2008; 18(2):148–68. [PubMed: 17960647]

Sabeti J, Nelson TE, Purdy RH, Gruol DL. Steroid pregnenolone sulfate enhances NMDA-receptor-independent long-term potentiation at hippocampal CA1 synapses: role for L-type calcium channels and sigma-receptors. Hippocampus. 2007; 17(5):349–69. [PubMed: 17330865]

Sabino V, Cottone P, Zhao Y, Steardo L, Koob GF, Zorrilla EP. Selective reduction of alcohol drinking in Sardinian alcohol-preferring rats by a sigma-1 receptor antagonist. Psychopharmacology (Berl). 2009; 205(2):327–35. [PubMed: 19440699]

Schummers J, Bentz S, Browning MD. Ethanol's inhibition of LTP may not be mediated solely via direct effects on the NMDA receptor. Alcohol Clin Exp Res. 1997; 21(3):404–8. [PubMed: 9161598]

Sinclair JG, Lo GF. Ethanol blocks tetanic and calcium-induced long-term potentiation in the hippocampal slice. Gen Pharmacol. 1986; 17(2):231–3. [PubMed: 3699450]

Slawecki CJ, Thorsell A, Ehlers CL. Long-term neurobehavioral effects of alcohol or nicotine exposure in adolescent animal models. Annals of the New York Academy of Sciences. 2004; 1021:448–52. [PubMed: 15251927]

Sommer WH, Rimondini R, Hansson AC, Hipskind PA, Gehlert DR, Barr CS, Heilig MA. Upregulation of voluntary alcohol intake, behavioral sensitivity to stress, and amygdala crhr1 expression following a history of dependence. Biol Psychiatry. 2008; 63(2):139–45. [PubMed: 17585886]

Spanagel R. Alcoholism: a systems approach from molecular physiology to addictive behavior. Physiol Rev. 2009; 89(2):649–705. [PubMed: 19342616]

Spear LP. The adolescent brain and age-related behavioral manifestations. Neuroscience and biobehavioral reviews. 2000; 24(4):417–63. [PubMed: 10817843]

Spruston N. Pyramidal neurons: dendritic structure and synaptic integration. Nat Rev Neurosci. 2008; 9(3):206–21. [PubMed: 18270515]

Staff NP, Spruston N. Intracellular correlate of EPSP-spike potentiation in CA1 pyramidal neurons is controlled by GABAergic modulation. Hippocampus. 2003; 13(7):801–5. [PubMed: 14620875]

Stefanski R, Justinova Z, Hayashi T, Takebayashi M, Goldberg SR, Su TP. Sigma1 receptor upregulation after chronic methamphetamine self-administration in rats: a study with yoked controls. Psychopharmacology (Berl). 2004; 175(1):68–75. [PubMed: 15029471]

Steffensen SC, Henriksen SJ. Effects of baclofen and bicuculline on inhibition in the fascia dentata and hippocampus regio superior. Brain Res. 1991; 538(1):46–53. [PubMed: 1850318]

Su TP, London ED, Jaffe JH. Steroid binding at sigma receptors suggests a link between endocrine, nervous, and immune systems. Science. 1988; 240(4849):219–21. [PubMed: 2832949]

Taube JS, Schwartzkroin PA. Mechanisms of long-term potentiation: EPSP/spike dissociation, intradendritic recordings, and glutamate sensitivity. J Neurosci. 1988; 8(5):1632–44. [PubMed: 2896764]

Thomas MJ, Mameli M, Carta M, Fernando Valenzuela C, Li PK, Partridge LD. Neurosteroid paradoxical enhancement of paired-pulse inhibition through paired-pulse facilitation of inhibitory circuits in dentate granule cells. Neuropharmacology. 2005; 48(4):584–96. [PubMed: 15755486]

Tokuda K, Zorumski CF, Izumi Y. Modulation of hippocampal long-term potentiation by slow increases in ethanol concentration. Neuroscience. 2007; 146(1):340–9. [PubMed: 17346891]

Turrigiano GG, Nelson SB. Homeostatic plasticity in the developing nervous system. Nat Rev Neurosci. 2004; 5(2):97–107. [PubMed: 14735113]

VanDoren MJ, Matthews DB, Janis GC, Grobin AC, Devaud LL, Morrow AL. Neuroactive steroid 3alpha-hydroxy-5alpha-pregnan-20-one modulates electrophysiological and behavioral actions of ethanol. J Neurosci. 2000; 20(5):1982–9. [PubMed: 10684899]

Wang M, He Y, Eisenman LN, Fields C, Zeng CM, Mathews J, Benz A, Fu T, Zorumski E, Steinbach JH, Covey DF, Zorumski CF, Mennerick S. 3beta - hydroxypregnane steroids are pregnenolone sulfate-like GABA(A) receptor antagonists. J Neurosci. 2002; 22(9):3366–75. [PubMed: 11978813]

Wang Z, Xu NL, Wu CP, Duan S, Poo MM. Bidirectional changes in spatial dendritic integration accompanying long-term synaptic modifications. Neuron. 2003; 37(3):463–72. [PubMed: 12575953]

White AM, Matthews DB, Best PJ. Ethanol, memory, and hippocampal function: a review of recent findings. Hippocampus. 2000; 10(1):88–93. [PubMed: 10706220]

White AM, Swartzwelder HS. Age-related effects of alcohol on memory and memory-related brain function in adolescents and adults. Recent developments in alcoholism. 2005; 17:161–76. [PubMed: 15789865]

Whittington MA, Faulkner HJ, Doheny HC, Traub RD. Neuronal fast oscillations as a target site for psychoactive drugs. Pharmacol Ther. 2000; 86(2):171–90. [PubMed: 10799713]

Xu J, Kang N, Jiang L, Nedergaard M, Kang J. Activity-dependent long-term potentiation of intrinsic excitability in hippocampal CA1 pyramidal neurons. J Neurosci. 2005; 25(7):1750–60. [PubMed: 15716411]

Zhang H, Cuevas J. Sigma receptors inhibit high-voltage-activated calcium channels in rat sympathetic and parasympathetic neurons. Journal of neurophysiology. 2002; 87(6):2867–79. [PubMed: 12037190]

Zhang H, Cuevas J. sigma Receptor activation blocks potassium channels and depresses neuroexcitability in rat intracardiac neurons. J Pharmacol Exp Ther. 2005; 313(3):1387–96. [PubMed: 15764734]

Zhang W, Linden DJ. The other side of the engram: experience-driven changes in neuronal intrinsic excitability. Nature reviews. 2003; 4(11):885–900.

Zucker RS, Regehr WG. Short-term synaptic plasticity. Annu Rev Physiol. 2002; 64:355–405. [PubMed: 11826273]

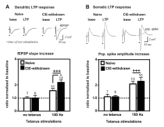

Figure 1.

Comparison of LTP magnitudes at dendritic synapses (A) and soma (B) of CA1 neurons in naïve versus CIE-withdrawn hippocampal slices. Top traces are evoked fEPSPs (A) and pop. spike signals (B) in a representative naïve control or CIE-withdrawn slice recorded at baseline (base) and 60 min after high-frequency stimulations (100 Hz, 1 s duration, 3 trains, 20 s inter-train interval). Test stimulations were applied at an intensity evoking the near half-maximal pop. spike response amplitude at baseline (applied voltage: naïve control, 15 ± 2 V and CIE-withdrawn, 15 ± 1 V). Dots denote the time of the test stimulations. Bar graphs represent the mean response magnitude at 55-60 min after or in the absence of the 100 Hz stimulations, as normalized to the mean baseline response (i.e., the ratio between the mean of 5 consecutive response magnitudes at the two time points). A ratio of 1 (dashed line) would indicate no change in the evoked response from baseline. Mean values ± SEM are shown for the indicated number of slices. +++, $p < 0.001$ no tetanus versus 100 Hz tetanus and *, $p < 0.05$ CIE-withdrawn versus Naive (100 Hz) by Bonferroni post t-test comparisons.

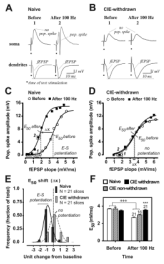

Figure 2.

CIE withdrawn hippocampal slices exhibit E-S dissociation with LTP. **A-B**, Concurrent somatic and dendritic recordings from a representative naïve control (A) or CIE-withdrawn (B) hippocampal slice, illustrating that in the former case, the fEPSP strength previously subthreshold for generating a pop. spike at baseline (1) is now capable of evoking a robust pop. spike signal after LTP induction (2; A), whereas in the latter case the E-S relationship at the subthreshold fEPSP strength remains unaltered after LTP induction (B). **C-D**, E-S coupling relationships before and at 60 min after 100 Hz stimulations for an individual naïve (C) or CIE-withdrawn (D) hippocampal slice. Data depict pop. spike amplitudes as a function of their corresponding dendritic fEPSP slopes evoked by increasing the applied stimulus voltage from subthreshold to maximal strengths (see Methods). Also shown are the fitted Boltzmann sigmoidal curves (R^2 = 0.9935-0.9952) and E_{50} values. Arrow denotes a leftward shift in the E_{50} from baseline (Δ x) consistent with E-S potentiation in the naïve slice (C), while overlapping E-S curves indicate no E-S potentiation in the CIE-withdrawn slice (D). Boxed data points in C and D are from the example waveforms shown in A and B, respectively. **E,** Frequency distribution of the E_{50} shift at 60 min after tetanization in naïve or CIE-withdrawn hippocampal slices. Negative values on the X-axis indicate leftward shifts in the E_{50} towards E-S potentiation in individual slices. Histograms depict the fraction of the total number of slices recorded that show a change in the E_{50} within the specified range. Units of change are in increments of 25% from the baseline E_{50}value (before tetanization): zero represents negligible change within ± 12.5% and '−1' represents a decrease by greater than −12.5% and less than −37.5% from baseline. Fitted curves illustrate the number of responses in the various E_{50} shift ranges that would be predicted by the Gaussian model for a normal distribution (solid and dashed curves: R^2 = 0.9947 and 0.9658, naïve and CIE-withdrawn, respectively). **F,** Mean E_{50} values before and at 60 min after LTP induction in naïve, CIE non-withdrawn and CIE-withdrawn slices. Data are the fitted E_{50} values derived from a single E-S curve generated by averaging the evoked pop spike amplitudes within certain incremental ranges of the incoming fEPSP slope at the two time points. Mean values ± SEM are shown for the indicated number of slices for each treatment group. +++, $p < 0.001$ 'before' versus 'after 100 Hz'. ***, $p < 0.001$ Naive versus CIE-withdrawn (after 100 Hz) by Bonferroni post t-tests corrected for multiple comparisons.

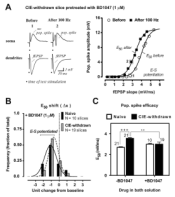

Figure 3.

Sigma-1 receptor antagonist BD1047 restores E-S potentiation in CIE-withdrawn hippocampal slices. Data are presented as described in Fig 2 legend. **A,** E-S coupling relationship before and at 60 min after 100 Hz stimulations for an individual CIE-withdrawn slice pretreated with BD1047 in the bath solution (1 μM; beginning at 30 min before and with continuous perfusion throughout the recording period). Boxed data points before (1) and after (2) tetanus stimulations are from the representative traces shown on the left. Note the leftward shift in the E-S curve after tetanization, consistent with E-S potentiation in this example. **B,** Frequency distribution of the E_{50} shift at 60 min after tetanization in BD1047 pretreated naïve or CIE-withdrawn slices. Also shown are the fitted Gaussian distributions (solid and dashed curves: $R^2 = 0.9655$ and 0.9938, pretreated naïve and CIE-withdrawn, respectively; see Fig. 2E legend for details). **C,** Mean E_{50} values at 60 min after LTP induction in naïve and CIE-withdrawn slices pretreated with BD1047 (1 μM; +BD1047). Data from slices not exposed to BD1047 (−BD1047 or ACSF only) are included from Fig. 2F for comparison. Mean values ± SEM are shown for the indicated number of slices. +++, $p < 0.001$ Naive versus CIE-withdrawn (no BD1047) and **, $p < 0.01$ CIE withdrawn −BD1047 versus +BD1047 by Bonferroni post t-test comparisons.

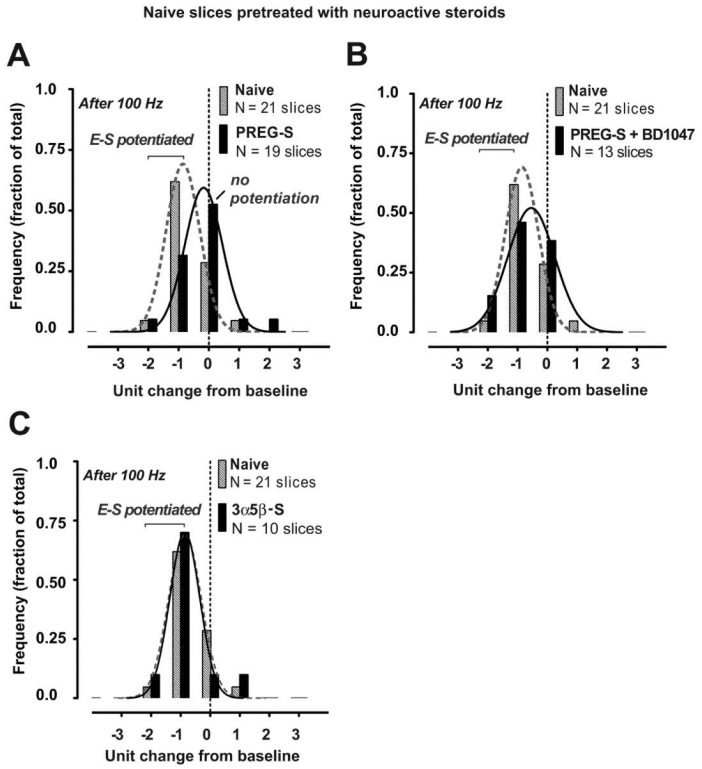

Figure 4.

Elevated concentrations of neurosteroid pregnenolone sulfate (PREG-S), but not neurosteroid 3α,5β sulfate, block activity-induced E-S potentiation in naïve slices via sigma-1 receptor mediated actions. **A-C,** Frequency distribution of the E_{50} shift at 60 min after tetanization in naïve slices pretreated with PREG-S alone (A, 5 μM) or in combination with BD1047 (B, 1 μM) or with 3α,5β sulfate alone (C, 5 μM). Drugs were applied beginning at 30 min before and with continuous perfusion throughout the recording period. Data from naïve control slices recorded in ACSF alone are included from Fig. 2E for comparison. Also shown are the fitted Gaussian distributions (solid and dashed curves: R^2 = 0.9748-0.9947). Negative values on the X-axis indicate leftward shifts in the E_{50} towards E-S potentiation in individual slices. Histograms depict the fraction of the total number of slices recorded that show a change in the E_{50} within the specified range. Units of change are in increments of 25% from the baseline E_{50}value (before tetanization) as described in Fig. 2E legend.

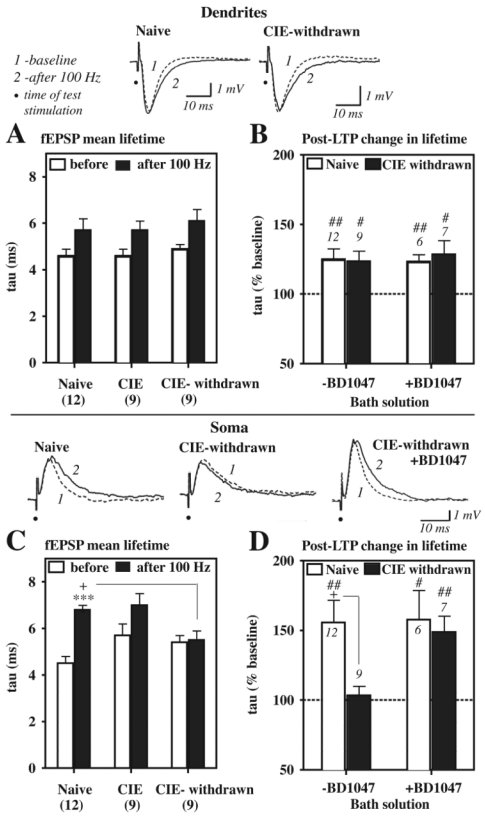

Figure 5.

fEPSP decay time course at CA1 soma is prolonged by LTP in naive control but not CIE-withdrawn slices. Data are decay time constants (tau or mean lifetime) for the evoked dendritic (A, B) and somatic (C, D) fEPSPs before (baseline) and at 60 min after the 100 Hz stimulations. Top traces are example fEPSP waveforms before (1, dashed curve) and after (2, solid curve) in a representative naïve or CIE-withdrawn slice. Note the slowing of the somatic fEPSP decay time course after LTP induction in the naive but not the CIE-withdrawn slice (first versus middle trace in bottom panel). **A, C,** Mean tau values for time-locked dendritic (A) and somatic (C) fEPSP signals in naïve control, CIE non-withdrawn ('CIE'), and CIE-withdrawn slices. fEPSPs near threshold were selected that were not contaminated by the presence of a pop. spike and matched with respect to their dendritic fEPSP slope for tau determinations. **B, D,** Mean percentage increase in the tau value at 60 min after LTP induction in slices pretreated (+) with BD1047 (1 μM), as compared to control slices not exposed to BD1047 (−BD1047) from data shown in A and C. Dashed line at 100% would indicate no change in the fEPSP mean lifetime from baseline. Data are the indicated number of slices from a subset recorded in Fig. 2E, 3B, and 5F. ##, $p < 0.01$ and #, $p < 0.05$ versus 100% by a one-sample t-test (B, D). ***, $p < 0.001$ naïve, 'before' versus 'after 100 Hz' (C). +, $p < 0.05$ Naive versus CIE-withdrawn (C and D).

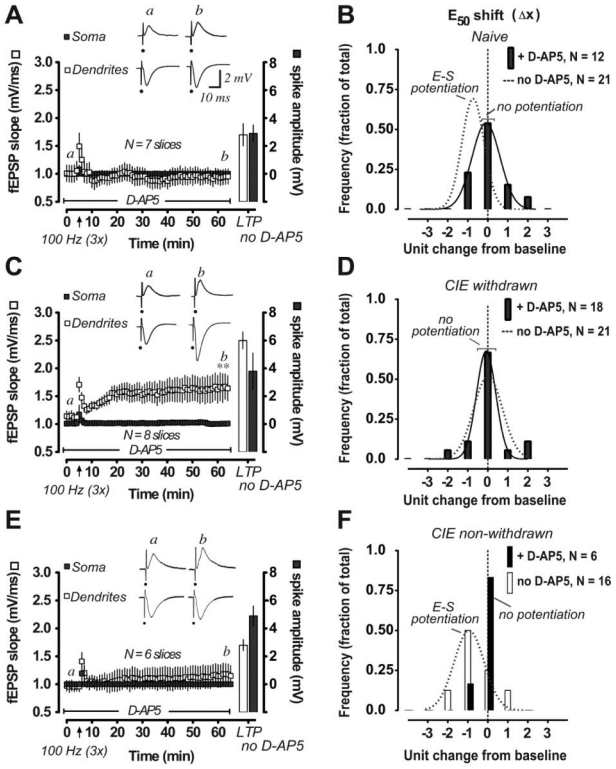

Figure 6.

Assessment of NMDA receptor function in naïve (A, B), CIE withdrawn (C, D) and CIE non-withdrawn (E, F) hippocampal slices during LTP and E-S potentiation. **A, C, E,** Time course of change in the concurrently recorded pop. spike amplitudes (closed rectangles and right Y-axis) and dendritic fEPSP slopes (open rectangles and left Y-axis) after 100 Hz stimulations (arrow, 3 trains) in the presence of D-AP5 in the bath solution (50 μM; beginning at 30 min before baseline recordings and with continuous perfusion throughout as indicated). Bars represent response magnitudes after a second set of 100 Hz stimulations were applied following a 30 min washout of D-AP5 with normal ACSF perfusion. Waveforms are representative somatic and dendritic recordings at the times indicated in the presence of D-AP5 (a, before and b, after tetanus). Data are mean values ± SEM for the indicated number of slices. **B, D, F,** Frequency distribution of the E_{50} shift at 60 min after tetanization in DAP5 pretreated slices (closed columns). Data are presented as described in Fig. 2 legend. Fitted Gaussian distributions are shown for the indicated number of slices when appropriate (solid curves: $R^2 = 0.979$ and 0.9537, naïve and CIE-withdrawn, respectively). Dashed curves in B and D represent the fitted distributions in naïve and CIE-withdrawn slices not pretreated with D-AP5 from data shown in Fig. 2E. Open columns and dashed curve in F represent the distribution of responses in a separate group of CIE non-withdrawn slices not pretreated with D-AP5. **, $p < 0.01$ fEPSP slope at 55-60 min after versus before 100 Hz by Bonferoni post t-tests corrected for multiple comparisons (C).

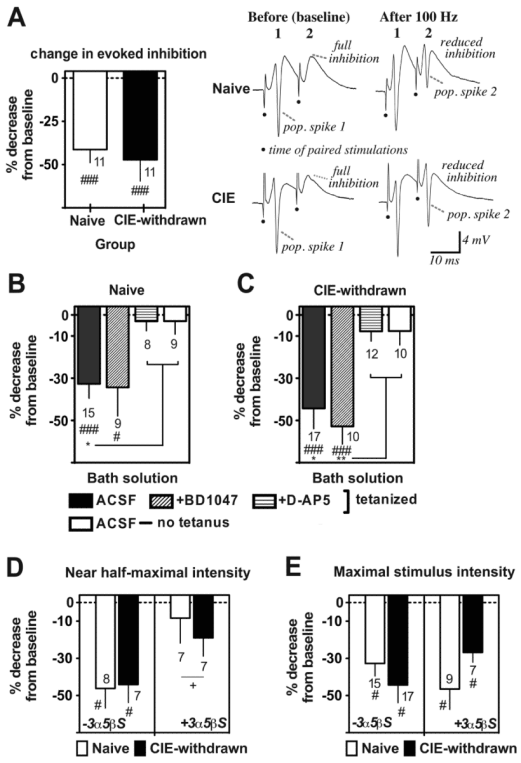

Figure 7.

Recurrent feedback inhibition is overcome by LTP in a NMDA receptor dependent manner for both naïve and CIE-withdrawn slices. Data are the percentage change from baseline in paired-pulse (10 ms) inhibition levels under various recording conditions. Dashed line at zero indicates no change and negative values on the Y-axis indicated reduced inhibition at 60 min after or in the absence of 100 Hz stimulations. **A,** Reduced paired-pulse inhibition at the maximal stimulation voltage in tetanized naive (E-S potentiated) and CIE-withdrawn (non E-S potentiated) slices. Data are from a subset of slices that fell in the peak of the E_{50} shift distributions shown in Fig. 2E (closed and slashed columns). Traces on the right are example somatic recordings from a representative naive or CIE-withdrawn slice, demonstrating complete abolition of the pop. spike signal by the paired-pulse stimulations at baseline and reduced inhibition at 60 min after the 100 Hz stimulations. Filled dots denote the time of the paired stimulations. **B-C,** Paired-pulse inhibition at the maximal stimulus voltage in tetanized control (ACSF, no drug), BD1047 (1 μM) or D-AP5 (50 μM) pretreated slices or in control (ACSF) slices where the tetanus stimulations were omitted. Filled columns here represent a combination of both E-S potentiated and non-potentiated slices within each group that fell over the entire E_{50} distribution range shown in Fig. 2E. **D-E,** Paired-pulse inhibition at the near half-maximal (D) or maximal (E) stimulus voltage in slices pretreated (+) or not (−) with 3α5β pregnanolone sulfate (3α5βS) in the bath solution (5 μM; at 30 min before and with continuous perfusion throughout recordings). Some data in E (no 3α5βS; first set of columns) are included from B and C (closed columns) for comparisons. Data are mean values ± SEM for the indicated number of slices. ###, $p < 0.001$ and #, $p < 0.05$ versus zero change from baseline by a one sample t-test (A-E). **, $p < 0.01$ and *, $p < 0.05$ ACSF ‘tetanized’ versus both ‘non-tetanized’ and ‘D-AP5 tetanized’ slices by Bonferroni post t-test comparisons (B-C). +, $p < 0.05$ ‘+3α5β sulfate’ versus ‘−3α5β sulfate’ by two-way ANOVA ($F_{2,25} = 8.2$; D).

Table1

Summary statistics from paired-pulse inhibition analyses in naïve control and CIE withdrawn hippocampal slices

Drug	Tetanus	Group	N	Paired-pulse Inhibition Maximal strength			N	Paired-pulse Inhibition Near half-maximal strength		
				Baseline	60 min	% change		Baseline	60 min	% change
ACSF	100 Hz	Naive	15	77.6 ± 6.4	55.1 ± 7.7	−32.7 ± 6.8###	8	71.9 ± 12.2	49.9 ± 10.4	−46.2 ± 10.6#
		CIE	17	63.3 ± 5.6+	39.1 ± 8.4+	−44.3 ± 9.6###	7	72.3 ± 4.4	46.7 ± 7.1	−44.1 ± 9.7#
ACSF	none	Naive	9	72.1 ± 10.0	66.6 ± 9.1	−3.0 ± 6.1*				
		CIE	10	74.5 ± 10.7	75.4 ± 10.1	−7.6 ± 6.6*				
D-AP5	100 Hz	Naive	8	68.6 ± 11.5	63.8 ± 8.3	−3.0 ± 4.5*	8	84.3 ± 13.6	69.5 ± 11.7	−4.8 ± 3.4*
		CIE	12	73.1 ± 13.3	70.5 ± 15.0	−7.7 ± 4.6*	9	69.7 ± 9.8	74.7 ± 8.2	−3.1 ± 5.2*
3α5β-S	100 Hz	Naive	9	76.0 ± 6.8	52.5 ± 12.2	−46.5 ± 11.0#	7	66.0 ± 7.7	52.1 ± 13.9	−8.4 ± 13.4*
		CIE	7	82.4 ± 9.6	70.8 ± 5.2*	−26.8 ± 5.3#	7	94.6 ± 3.5+	76.8 ± 10.2+*	−19.0 ± 9.8*
BD1047	100 Hz	Naive	9	64.8 ± 9.9	50.1 ± 13.2	−34.3 ±13.5#				
		CIE	10	64.9 ± 11.4	40.9 ± 12.3	−52.8 ± 8.3###				

Mean percentage inhibition (2nd versus 1st pop. spike amplitude) values ± SEM at baseline and 60 min with or without 100 Hz tetanus stimulations in ethanol-naïve (Naïve) or CIE-withdrawn (CIE) hippocampal slices recorded under the conditions indicated (*N* number of slices). Data are from slices that exhibited at least ~30-40% initial paired-pulse (10 ms inter-pulse interval) inhibition during stability tests. Drugs indicated were added to the flow of the ACSF bath solution at 30 min prior to baseline and for the remaining duration of the recordings (3α5β3-S 5 μM; D-AP5 50 μM; BD1047 1 μM). % change indicates the decrease in paired pulse inhibition at 60 min relative to the baseline value using within-slice comparisons such that greater negative values indicate stronger disinhibition by LTP.

# $p < 0.05$

$p < 0.001$ versus no change by a one-sample t-test.

+ $p < 0.05$ main effect of CIE treatment versus matched naïve control across both time points by 2-way ANOVA;

* $p < 0.05$ versus matched ACSF (no drug), 100 Hz by a Bonferroni t-test comparison.